DMD Fast Forward. Published on October 16, 2013 as doi:10.1124/dmd.113.053884

DMD#53884

Deoxyschizandrin, a Naturally Occurring Lignan, is a Specific Probe Substrate of Human Cytochrome P450 3A

Jingjing Wu, Yunfeng Cao, Yanyan Zhang, Yong Liu, James Y. Hong, Liangliang Zhu, Guangbo Ge, Ling Yang

Laboratory of Pharmaceutical Resource Discovery, Dalian Institute of Chemical Physics, Chinese Academy of Sciences, 457 Zhongshan Road, Dalian, China (J.W., Y.C., Y.Z., Y.L., L.Z., G.G., L.Y.);

Department of Biopharmaceutical Sciences, University of Illinois, Chicago, USA (J.Y.H.);

Shanghai Institute of Planned Parenthood Research, Shanghai, 200032, China (Y.C.);

Graduate University of Chinese Academy of Sciences, Beijing, China (J.W., L.Z.)

Running title: Deoxyschizandrin Hydroxylation by CYP3A

Corresponding Author:

Dr. Ling Yang,

Laboratory of Pharmaceutical Resource Discovery, Dalian Institute of Chemical Physics, Chinese Academy of Sciences, 457 Zhongshan Road, Dalian, China.

E-mail: yling@dicp.ac.cn. Telephone: (86) 411 84379317; Fax: (86) 411 84676961

Document Statistics:

Text Pages: 42

Tables: 3

Figures: 5

References: 37

Abstract: 249 words

Introduction: 727 words

Discussion: 1500 words

Abbreviations:

DS, deoxyschizandrin; ISZ, isoschizandrin; HLM, human liver microsomes; RLM, Wistar rat liver microsomes; NADPH, nicotinamide-adenine dinucleotide phosphate; CYP, cytochrome P450; TST, testosterone; 6β-HTS, 6β-hydroxytestosterone; NIF, nifedipine; OX-NIF, oxidized nifedipine; MDZ, midazolam; 1′-OH-MDZ, 1′-hydroxymidazolam; ABT, 1-Aminobenzotriazole; TEPA, triethylenethiophosphoramide; UFLC-DAD, ultra-fast liquid chromatography-diode array detector; ESI-MS, electrospray ionization-mass spectrometry; V_{max}, apparent maximum reaction velocity; K_m, apparent affinity; CL_{int}, intrinsic clearance;

NMR, nuclear magnetic resonance.

Abstract

To accurately predict the modifications done during metabolic processes by Cytochrome P450 (CYP) 3A enzyme, selecting substrates that best represent a broad range of substrate substitutions and that follow the Michaelis-Menten kinetic properties is highly necessary. In the present study, the oxidative pathways of deoxyschizandrin (DS), the most abundant lignan in *Fructus Schisandrae* fruit extract, were characterized with liver microsomes from human (HLM) and rat (RLM). Only one mono-hydroxylated metabolite 7(*S*)-hydroxylated metabolite (isoschizandrin, ISZ) was identified using LC-MS and NMR techniques. CYP3A4 and CYP3A5 were found to be the major isoforms involved in the mono-hydroxylation of DS. Also, the kinetic studies showed that DS hydroxylation obeyed the Michaelis-Menten kinetics both in HLM and in RLM. However, the subsequent metabolism of ISZ was nearly non-existent when DS was present. More importantly, the interactions between DS and three well-characterized CYP3A probe substrates, testosterone (TST), midazolam (MDZ), and nifedipine (NIF), were studied. TST and MDZ were shown to compete with DS for the mutual binding site, causing K_m to be increased. The presence of DS also lowered the binding affinities for MDZ and TST. However, DS showed only slight inhibitory effects on nifedipine (NIF) oxidation even though NIF was able to inhibit DS hydroxylation in a noncompetitive fashion. These results show that DS is a good representative substrate of MDZ and TST primarily due to their shared, large binding regions on CYP3A. Therefore, DS is an attractive candidate as a novel CYP3A probe substrate for predicting the metabolic modifications in CYP3A activity.

Introduction

Cytochrome P450 (CYP) 3A, the most abundant human P450 enzyme, is involved in the metabolism of many structurally diverse therapeutic agents (Wienkers and Heath, 2005). As a consequence the individual variability or metabolic modification in CYP3A activity has a potential to greatly increase the risk of drug toxicity when a drug is administrated alone or as a part of combination therapy, especially for those with narrow therapeutic windows (Frye, 2004; Kalgutkar et al., 2007). Thus, a "probe" compound, which can be metabolized exclusively by an individual CYP enzyme, is in great necessity in order to evaluate the metabolic clearance rate for dosage adjustment and to assess the alteration of the CYP activities in clinical settings where there are high risks for drug-drug interactions (DDI) (Zhou et al., 2007; Wille et al., 2008).

To date, many *in vitro* probe substrates for CYP have been established to evaluate the potential for a new drug to modify CYP activities based on the *in vitro* probe reactions (Kenworthy et al., 1999; Yuan et al., 2002). However, the available information indicated that the substrate-differential response was often observed for CYP3A4. For example, haloperidol, activates dextromethorphan N-demethylation, but inhibits nifedipine oxidation (Yuan et al., 2002); erlotinib stimulates the midazolam 1'-hydroxylation, but inhibits the formation of 6β-hydroxytestosterone and oxidized nifedipine (Dong et al., 2011). Stresser et al. showed that the extent of substrate dependence for the quantitative inhibition parameters (IC_{50}) is as large as 195-fold among the tested CYP3A4 reactions (Stresser et al., 2000).

Several reasons could partly explain the phenomena mentioned above. Firstly, the presence of several distinct binding domains within the CYP3A active site results in various

DMD Fast Forward. Published on October 16, 2013 as DOI: 10.1124/dmd.113.053884
This article has not been copyedited and formatted. The final version may differ from this version.

substrate subgroups (Galetin et al., 2005). Expectedly, false negative prediction of DDI will probably occur between two different subgroups of substrates due to the lack of mutual binding site. Secondly, in most cases, the CYP-catalyzed reactions can be described using the Michaelis-Menten equation based on the premise that substrate-enzyme interactions occur at only one site per enzyme. Then estimates can be deduced using V_{max} and K_m parameters to predict both clearance and DDI *in vivo* (Lin and Lu, 1997; Houston and Kenworthy, 2000). Yet, due to the relatively large substrate-binding cavity of CYP3A, two or more molecules of smaller substrates are postulated to simultaneously occupy the active site cavity (Yano et al., 2004). In response, more complex and rational mechanistic analyses are demanded (Galetin et al., 2003); otherwise, false positive or negative prediction of DDI will result from classical Michaelis-Menten analysis. Finally, the uniqueness of catalytic site within the substrate-binding cavity of CYP3A that help yield a single metabolite is indispensable to accurately quantify the total intrinsic metabolic clearance.

Unfortunately, until now, most of the commonly used *in vitro* probes are reported to demonstrate non-Michaelis-Menten kinetic properties, such as auto-activation for testosterone, a probe used in 50% reported studies, and auto-inhibition for midazolam (Houston and Kenworthy, 2000). Therefore, a criteria-based screening for better probe substrates that demonstrate Michaelis-Menten kinetics with a single metabolite and excellent substrate substitution properties, are highly sought since they can serve as the most representative *in vitro* probes for CYP3A metabolic activity

Previously, our lab has screened the CYP3A substrates from a large number of Traditional Chinese Medicines that classified as superior drugs (Wu et al., 2012). *Fructus Schisandrae*

has been used for thousands of years, owing to its diverse pharmacological effects (Wei et al., 2010). Many structurally similar dibenzocyclooctadiene lignans from *Fructus Schisandrae* were found to be metabolized by CYP3A4. For example, schizandrin has been proved to undergo C-8 hydroxylation and subsequent demethylation by CYP3A4 *in vitro* (Cao et al., 2010). Also, our preliminary experiments indicated that deoxyschizandrin (DS), another most abundant lignan from*Fructus Schisandrae*, was metabolized to a single metabolite via CYP3A4. Besides, it is worthy to note the similarity of chemical structures between DS and schizandrin, which is differed by a single hydroxyl group present on the cyclooctene ring. Therefore, we hypothesized that DS might be a novel CYP3A substrate that caters for the desired criteria of *in vitro* probe.

The aim of the present study was therefore to find further support that DS may serve as a specific probe substrate for CYP3A *in vitro*, through identifying its metabolite, metabolic pathway, and specificity to CYP3A. Then further to assess DS metabolic kinetic property and its substrate substitution for three commonly used subgroup probes testosterone, midazolam and nifedipine.

DMD Fast Forward. Published on October 16, 2013 as DOI: 10.1124/dmd.113.053884
This article has not been copyedited and formatted. The final version may differ from this version.

Materials and methods

Chemicals. DS (purity > 98.0%) was purchased from China Chengdu Scholar Bio-Tech. CO., LTD. 1-Aminobenzotriazole (ABT), sulfaphenazole, quinidine, clotrimazole, clomethiazole, furafylline, 8-methoxypsoralen, omeprazole, testosterone (TST), 6β-hydroxytestosterone (6β-HTS), nifedipine (NIF), oxidized nifedipine (OX-NIF), midazolam (MDZ), 1′-hydroxymidazolam (1′-OH-MDZ), glucose-6-phosphate dehydrogenase, $NADP^+$, and D-glucose-6-phosphate were purchased from Sigma-Aldrich (St. Louis, MO, USA). Ketoconazole was obtained from ICN Biomedicals Inc. (Aurora, Ohio, USA). Montelukast was from Beijing Aleznova Pharmaceutical (Beijing, China). Triethylenethiophosphoramide (thioTEPA) was purchased from Acros Organics (Geeleu, Belgium). All other reagents were of HPLC grade or of the highest grade commercially available.

Animals. Wistar rats (n=10, male, 180 to220 g) were purchased from Dalian Medical University (Dalian, China). The animals had free access to tap water and pellet diet (from the Experimental Animal Center of Dalian Medical University, Dalian, China) at a temperature of 20-25 °C with a 12-h light–dark cycle and relative humidity of 50±10%. All procedures involving animals complied with the Laboratory Animal Management Principles of China.

Enzyme source. Pooled human liver microsomes were obtained from Celsis *in Vitro* Technologies (USA). cDNA-expressed recombinant human CYP3A4 and CYP3A5 were obtained from Cypex Ltd. (Dundee, UK). cDNA-expressed CYP1A2, CYP2A6, CYP2B6, CYP2C8, CYP2C9, CYP2D6, CYP2E1, CYP3A1 and CYP3A2 derived from baculovirus-infected insect cells coexpressing NADPH-CYP reductase were obtained from BD Gentest Corp. (Woburn, MA, USA). cDNA-expressed CYP2C19 in Escherichia coli

coexpressing NADPH-CYP reductase was purchased from New England Biolabs Ltd. (Beijing, China). Pooled Wistar male rat liver microsomes (RLM, n=10) were prepared from liver tissue by differential ultracentrifugation as described previously (Liu et al., 2009), and the Lowry method was adopted to determine the concentration of microsomal protein by using bovine serum albumin as a standard (Lowry et al., 1951). Pooled mouse microsomes (MLM), pig microsomes (PLM), and male New Zealand rabbit microsomes (RaLM) were purchased from Research Institute for Liver Diseases (Shanghai, China). All microsomal samples and recombinant human CYP isoforms were stored at -80ºC until use.

Incubation conditions. The optimal conditions for microsomal incubation were determined in the linear range for the formation of metabolite from DS or ISZ. The incubation mixture, with a total volume of 200 µl, consisted of 100 mM potassium phosphate buffer (pH 7.4), NADPH-generating system (1 mM $NADP^+$, 10 mM glucose-6-phosphate, 1 unit/ml of glucose-6-phosphate dehydrogenase, and 4 mM $MgCl_2$), and liver microsomes. In all experiments, DS or ISZ (20mM previously dissolved in methanol) was serially diluted to the required concentrations, where the final methanol concentration did not exceed 0.5% (v/v) in the mixture. After 3 min of incubation at 37°C, the reaction was initiated by adding NADPH-generating system and further incubated for 10 min at 37°C in a shaking water bath. The reaction was terminated by the addition of methanol (200 µl). The mixture was kept on ice until it was centrifuged at 20,000× g for 10 min at 4°C. Aliquots of supernatants were stored at -30°C until analysis. Control incubations without NADPH or without substrate or without microsomes were carried out to ensure that the formation of metabolite was microsomes- and NADPH-dependent. All incubations throughout the study were carried out

in three independent experiments performed in duplicate with standard deviation (S.D.) values generally below 10%, and results were expressed as mean ± S.D.

Liver Perfusion Studies. Male Wistar rats were anaesthetised with intraporitoneal administration of sodium pentobarbital (50 mg/kg). The surgical procedure was based on previously described methods with minor modification (Liu et al., 2000); Erythrocyte-free Krebs-Hensenleit buffer (KHB) that was oxygenated with 95% O_2 and 5% CO_2. After anesthesia, the abdomen was opened with a U-section. The hepatic artery and infrahepatic vena cava were ligated, and the portal vein was cannulated by a 14-gauge needle double catheter for infusion. The venous perfusate outflow was allowed to drain back into the reservoir. KHB without DS perfusate passed the liver at a flow rate of 15ml/min at 37°C for 20 min for equilibration. Then, KHB perfusate, containing DS (50 μM) from a second reservoir with 200ml, was used for recirculation for 30 min. The reservoir perfusate sample was sampled at the end of the experiment and stored at -20°C before assay.

UFLC-DAD and UFLC-ESI-MS analysis. The UFLC system was employed. An ODS analytical column (100 mm × 2.1 mm, 3 μm, Thermo) with an ODS guard column (150 nm × 2.1 mm, 3 μm, Thermo) was used to separate DS, MDZ, TST, NIF, ISZ and their respective metabolites. As for DS, MDZ, TST and NIF, the mobile phase consisted of methanol (A pump) and water (B pump) with the following gradient profile: 0–9 min, 50%–5% B; 9-12 min, 5% B; 12–16.5 min, balanced to 50% B; As for ISZ, the mobile phase consisted of CH_3OH (A) and water with the following gradient profile: 0–12 min, 55%–45% B; 12-14 min, 45%–5% B; 14–18.5 min, balanced to 55% B. The flow rate was 0.25 ml/min and the column temperature was kept at 40ºC. The respective metabolites of DS, MDZ, TST and NIF

DMD Fast Forward. Published on October 16, 2013 as DOI: 10.1124/dmd.113.053884
This article has not been copyedited and formatted. The final version may differ from this version.

were detected at the detector wavelength of 250 nm, 254 nm, 245nm and 237 nm, respectively. Shimadzu LC-MS-2010EV (Kyoto, Japan) instrument with an ESI interface was used for identification of DS and its metabolite. Mass detection was performed in both positive-ion mode (ESI+) and negative ion mode (ESI-) from m/z 100 to 800. The detector voltage was set at +1.75 kV and –1.55 kV for positive and negative ion detections, respectively. The curved desolvation line temperature (CDL) and the block heater temperature were both set at 250ºC. Other MS detection conditions were as follows: interface voltage, 4 kV; CDL voltage, 40 V; nebulizing gas (N_2) flow was 1.5 L/min and the drying gas (N_2) pressure was set at 0.06 MPa. Data processing was performed using the LC-MS Solution version 3.41 software. DS, MDZ, TST, NIF and their respective metabolites were quantified by the standard curve of authentic standards, which was linear from 0.1 to 30 μM, with correlation coefficient of >0.999. The quantitative method displayed good sensitivity. The limit of detection for DS hydroxylated metabolite is 0.5 ng. The method also displayed good reproducibility, with the intra-day and inter-day variance both less than 3%.

Metabolite purification. The metabolite (ISZ) were biosynthesized using mixed liver microsomes from rat and human (90% RLM and 10% HLM) and purified for structure elucidation and quantitative analysis. In brief, the incubation system was scaled up to 50 ml. DS (20mM) was incubated with mixed liver microsomes (10 mg protein/ml) and NADPH-generating system (1mM $NADP^+$, 10 mM glucose-6-phosphate, 1 unit/ml of glucose-6-phosphate dehydrogenase, and 4 mM $MgCl_2$) for 90 min at 37 °C. Under these conditions, about 54% of DS was converted to the metabolite. Methanol (25ml) was added to the reaction mixture to precipitate the protein. After centrifuged at 9000 × *g* for 10 min, the

DMD Fast Forward. Published on October 16, 2013 as DOI: 10.1124/dmd.113.053884
This article has not been copyedited and formatted. The final version may differ from this version.

supernatant was separated and extracted with chloroform (50 ml ×3). The organic layer was combined and dried in vacuum. Then the residue was dissolved in methanol (1ml) and the metabolite was isolated and purified by semi-preparative HPLC with an YMC ODS-A column (10×250 mm, 5μm) and eluted with MeOH-H_2O (55:45, v/v) to give the compound M (8 mg). The purity of the metabolite was about 98% (HPLC).

NMR spectroscopy. ^{1}H and ^{13}CNMR spectra were obtained at 600 MHz on a Bruker AV-600 spectrometer (Bruker, Newark, Germany). Compound M were dissolved in $CDCl_3$ and experiments were conducted at 21 °C. Chemical shifts are reported in ppm with reference to tetramethylsilane.

Chemical inhibition study. Chemical inhibition studies were performed by adding different human CYP inhibitors to the incubation mixture of DS (2μM) before the addition of NADPH-generating system. The selection of a 2 μM concentration was based on the *K*m value. The selective inhibitors and their concentrations were as follows (Bjornsson et al., 2003): montelukast (5 μM) for CYP2C8 (Walsky et al., 2005), sulfaphenazole (10 μM) for CYP2C9, omeprazole (20 μM) for CYP2C19, quinidine (10 μM) for CYP2D6, clomethiazole (50 μM) for CYP2E1, ketoconazole (1 μM) for CYP3A4. Inhibition by furafylline (10 μM) for CYP1A2, 8-methoxypsoralen (2.5 μM) for CYP2A6, thioTEPA (50 μM) for CYP2B6 (Rae et al., 2002) and ABT (500 μM) for broad CYPs (Emoto et al., 2003) were examined by adding DS after preincubation with NADPH-generating system at 37°C for 10 min.

Clotrimazole (Turan et al. 2001) was found to be a selective inhibitor of rat CYP3A subfamily. Ketoconazole is a broad inhibitor for rat CYPs. Furafylline (Eagling et al. 1998) was able to inhibit both rat CYP1A and rat CYP2C. Therefore, inhibitory effects of

DMD Fast Forward. Published on October 16, 2013 as DOI: 10.1124/dmd.113.053884
This article has not been copyedited and formatted. The final version may differ from this version.

clotrimazole (0.001, 0.01, 0.1 μM), ketoconazole (1 μM), and furafylline (50 μM) towards DS metabolism in RLMs were examined.

Correlation study. The formation rate of the metabolite described for DS (2 μM, near K_m value) was determined in a panel of HLM prepared from 12 different human organ donors. These values were compared with the catalytic activities of CYP1A2, 2A6, 2C8, 2C9, 2C19, 2D6, 2E1, and 3A4. Isoform-specific reaction markers and the methods involved were as follows: phenacetin O-deethylation (CYP1A2), coumarin 7-hydroxylation (CYP2A6), paclitaxel 6α-hydroxylation (CYP2C8), diclofenac 4'-hydroxylation (CYP2C9), S-mephenytoin 4'-hydroxylation (CYP2C19), dextromethorphan O-demethylation (CYP2D6), chlorzoxazone 6-hydroxylation (CYP2E1) and testosterone 6β-hydroxylation (CYP3A4). The correlation parameter was expressed by the linear regression coefficient (r^2). A *p* value less than 0.05 was considered statistically significant.

Assay with recombinant CYPs. Ten cDNA-expressed human CYP isoforms co-expressing NADPH-P450 reductase and cytochrome b_5 (CYP1A2, CYP2A6, CYP2B6, CYP2C8, CYP2C9, CYP2C19, CYP2D6, CYP2E1, CYP3A4 and CYP3A5) were used. The incubations were carried out as described for the human liver microsomal study. To investigate the contribution of each CYP isoform, DS (50 μM) was incubated with each of the recombinant CYPs (40-80 nM) at 37°C for 20 min. UFLC-DAD was employed to monitor possible metabolites.

Kinetic study. To estimate kinetic parameters, DS (0.2-50μM) was incubated with the pooled HLM (0.05 mg protein/ml), pooled RLM (0.2 mg protein/ml), recombinant CYP3A4 or CYP3A5 (10 nM), CYP3A1 (0.1 mg CYP/ml) or CYP3A2 (0.075 mg CYP/ml) for 10min,

DMD Fast Forward. Published on October 16, 2013 as DOI: 10.1124/dmd.113.053884
This article has not been copyedited and formatted. The final version may differ from this version.

respectively. To compare DS kinetic parameters with those of the well-known CYP3A4 probes, TST, NIF and MDZ were simultaneously incubated with the pooled HLM, RLM, recombinant CYP3A4 or CYP3A5 for 10 min. On the basis of a previously reported document, reaction mixtures with human microsomes were incubated at 0.25, 0.25, 0.25 mg/ml of microsomal protein for TST, NIF and MDZ, respectively (Patki et al., 2003). Likewise, the kinetic study of ISZ metabolism was also conducted in HLM and RLM. ISZ (5-300 μM) was incubated with HLM (0.4 mg/ml) or with RLM (0.4 mg/ml) at 37°C for 30 min with NADPH-generating system. Formation of metabolites with liver microsomes was linear with respect to incubation time and microsomal protein concentration over ranges relevant to this study. All incubations were carried out in duplicate. The apparent K_m and V_{max} values were calculated from nonlinear regression analysis of experimental data according to the Michaelis-Menten equation with Origin version 7.5 software. Kinetic constants were reported as the value ± S.D. of the parameters estimate.

Interaction studies

Incubation conditions. Recombinant human CYPs at final concentrations of 20 nM were incubated with various concentrations of a pair of CYP3A substrates in 100 mM potassium phosphate buffer (pH 7.4) with 1 mM EDTA, 6 mM MgCl2, and an NADPH-generating system consisting of 1 mM $NADP^+$, 10 mM glucose-6-phosphate, 1 unit/ml of glucose-6-phosphate dehydrogenase, and 4 mM $MgCl_2$ in a total volume of 0.1 ml. Incubations were carried out in a 37°C shaking water bath for 10 min. The substrates (concentration ranged at least from 1/5 K_m to 5 K_m) were added to each incubation in either methanol or phosphate buffer depending on the solubility. The final concentration of the

DMD Fast Forward. Published on October 16, 2013 as DOI: 10.1124/dmd.113.053884
This article has not been copyedited and formatted. The final version may differ from this version.

organic solvent (methanol) in incubation media was ≤ 0.5% (v/v). The range of the inhibitor concentrations applied was from 0.5 to100 μM in most studies. The reaction was terminated by 100 μl of ice-cold methanol. Samples were then centrifuged at 20,000 g for 15 min and further analyzed by UFLC.

Inhibition kinetics analysis. Inhibition constant (K_i) values were determined by using various concentrations of substrates in the presence or absence of inhibitors with Origin version 7.5 software. When DS was used as the substrate, single-site kinetic model was used to calculate K_i values by nonlinear regression by using the equations for competitive inhibition (eq. 1), noncompetitive inhibition (eq. 2), or mixed inhibition (eq. 3) (Copeland, 2000; Liu et al., 2010).

$$v = \frac{V_{max} S}{K_m (1 + I / K_i) + S} \quad (1)$$

$$v = \frac{V_{max} S}{(K_m + S)(1 + I / K_i)} \quad (2)$$

$$v = \frac{V_{max} S}{K_m (1 + I / K_i) + S(1 + I / \alpha K_i)} \quad (3)$$

Here v is the velocity of the reaction; S and I are the substrate and inhibitor concentrations, respectively; K_i is the inhibition constant describing the affinity of the inhibitor for the enzyme; and K_m is the substrate concentration at half of the maximum velocity (V_{max}) of the reaction. The α value determines the degree to which the binding of inhibitor changes the affinity of the enzyme for substrate. When α is very large (α >1), binding of inhibitor prevents binding of the substrate and the mixed-model becomes identical to competitive inhibition. The type of inhibition was determined from the fitting of data to the enzyme inhibition models. Goodness of fit to kinetic and inhibition models was assessed from the r^2 values and

DMD Fast Forward. Published on October 16, 2013 as DOI: 10.1124/dmd.113.053884
This article has not been copyedited and formatted. The final version may differ from this version.

parameter S.D. estimates. Kinetic constants are reported as the mean ± S.D. of the parameter estimate.

Two-site kinetic models were used to calculate K_i values by using the equations for a substrate with substrate inhibition kinetics (eq. 4), and a substrate with sigmoidal kinetics (eq. 5) (Galetin et al., 2003).

$$v = \frac{V_{max}\left(\frac{S}{K_S} + \frac{\beta S^2}{K_S^{\,2}} + \frac{\gamma SI}{\delta K_S K_i}\right)}{1 + \frac{S}{K_S} + \frac{S^2}{K_S^{\,2}} + \frac{2SI}{\delta K_S K_i} + \frac{2I}{K_i} + \frac{I^2}{K_i^{\,2}}} \qquad (4)$$

In eq. 4, β represents change in product formation from SES complex due to the second substrate binding; γ represents change in product formation from IES complex due to inhibitor binding; and δ represents change in affinity of SE/ES complex for the inhibitor molecular.

$$v = \frac{V_{\max}\left(\frac{\mathrm{S}}{\mathrm{K}_S} + \frac{S^2}{\varepsilon K_S^{\,2}}\right)}{1 + \frac{2S}{K_S} + \frac{S^2}{\varepsilon K_S^{\,2}} + \frac{I}{K_i} + \frac{2SI}{\delta K_i K_S} + \frac{S^2 I}{\delta K_i K_S^{\,2}}} \qquad (5)$$

In eq. 5, δ represents change in affinity of SE/ES and SES complexes for the inhibitor molecular; ε represents change in affinity of SE/ES complex for the second substrate molecular.

DMD Fast Forward. Published on October 16, 2013 as DOI: 10.1124/dmd.113.053884
This article has not been copyedited and formatted. The final version may differ from this version.

Results

Identification of DS hydroxylation. A single new peak was eluted at 6.8 min by UFLC when DS (50 μM) was incubated with HLM and RLM (0.2 mg/ml) in the presence of NADPH for 20 min (Figure 1). Similar profiles were also observed in MLM, PLM and RaLM (Supplemental Figure 1). The peak was not detected in control samples without microsomes, NADPH or DS (data not shown). To identify the *in vivo* metabolic profile of DS, the rat liver perfusion was conducted to imitate the *in vivo* situation. As expected, one predominant metabolite was detected in the perfusate after 30 min (Figure 1). Mass spectra with positive ion ESI were dominated by $[M + K]^+$. The metabolite (M) was identified by UFLC-DAD-ESI-MS to show an *m/z* value of 471, a value that corresponds well to DS (416 plus 39) incorporated with the *m/z* 16 of the oxygen substitution (Supplemental Table 1). The monohydroxylated metabolite of DS was biosynthesized and purified for structure elucidation, as well as for the use as a standard in different analyses. The metabolite structure determination was carried out by NMR, using both ^{1}H-NMR and ^{13}C-NMR analyses (Table 1). And the most distinctive spectra changes were involved in the C-7 region. The doublet of C-7-methyl (C-17) proton signal at 1.00 ppm (3H, d) in DS was replaced by the singlet and shifted downfield to 1.1 ppm (3H, d) in the metabolite. Moreover, the ^{13}C-NMR spectrum of the metabolite showed C-7 downfield shift of 18.9 ppm, compared with DS. The above observations clearly indicated hydroxylation at C-7. ^{1}H- and ^{13}C-NMR spectra of the metabolite coincided with those of isoschizandrin standard (Ikeya et al., 1991). Additionally, no conjugates were observed in the UDP-glucuronic acid (UDPGA)-, 3'-Phosphoadenosine-5'-phosphosulfate (PAPS)- and S-Adenosyl-L-methionine

(SAM)-generating systems, when DS was incubated with either HLM or S9 fractions (data not shown).

Biotransformation of isoschizandrin by liver microsomes. To elucidate the subsequent biotransformation of ISZ (7S, 8R), a natural enantiomer of schizandrin (7R, 8R), ISZ was biosynthesized by the incubation of DS and NADPH-generating system in mixed liver microsomes. Four product peaks were observed when ISZ (100 μM) was incubated with the hepatic microsomes from human or rat (0.4 mg protein/ml) along with the NADPH-generating system for more than 30 min (Figure 1). Each metabolite of ISZ was below the detection limit when the incubation time is less than 25 min. These four metabolites (M-1, M-2, M-3 and M-4) were identified as demethylated ISZ by UFLC-ESI-MS (Supplemental Table 1), and the formation of these metabolites was time-, NADPH-, and microsome-dependent (data not shown). Demethylation was identified as the major metabolic pathway of ISZ, while, hydroxylation was the key metabolic pathway of schizandrin (Cao et al., 2010). Furthermore, no conjugates were observed in the UDP-glucuronic acid (UDPGA)-, 3'-Phosphoadenosine-5'-phosphosulfate (PAPS)- and S-Adenosyl-L-methionine (SAM)-generating systems, when ISZ was incubated with either HLM or S9 fractions (data not shown).

Chemical inhibition studies. The effect of various chemical inhibitors on the metabolism of DS was investigated in pooled HLM and RLM (Figure 2). ABT, a broad CYP inactivator, inhibited DS mono-hydroxylation completely, suggesting that CYPs were the enzymes responsible for DS hydroxylation. Among the ten selective inhibitors tested, ketoconazole, the selective inhibitor of CYP3A inhibited ISZ formation from DS by 100% ($p<0.05$). In our

DMD Fast Forward. Published on October 16, 2013 as DOI: 10.1124/dmd.113.053884
This article has not been copyedited and formatted. The final version may differ from this version.

experiments, the other putative inhibitors were not active in reducing DS metabolism in our in vitro test systems. These data together demonstrated that DS metabolism is catalyzed by CYP3A.

To explore whether the metabolic enzymes responsible for DS hydroxylation in rat were also CYP3A isoenzymes, inhibition studies in RLM were conducted with clotrimazole as a selective inhibitor for CYP3A, furafylline as the inhibitor for CYP1A and CYP2C, and ketoconazole as a broad inhibitor for rat CYPs. As illustrated in Figure 2, furafylline (50 μM) slightly inhibited the formation of ISZ in rat, whereas ketoconazole (1 μM) was able to inhibit the formation of ISZ nearly completely, and clotrimazole (0.1μM) also can inhibit the hydroxylation of DS completely. This result implied that CYP3A also played an important role in the hydroxylation of DS in rat.

Assay with recombinant human CYP isoforms. To elucidate CYP isoforms involved in the metabolism of DS in human, the activity of DS hydroxylation was determined in ten cDNA-expressed CYP isoforms (Figure 3). After incubation at 37°C for 20 min, hydroxylated metabolite ISZ was observed exclusively in CYP3A4 and CYP3A5. No metabolites were observed in the incubation with CYP1A2, CYP2A6, CYP2B6, CYP2C8, CYP2C9, CYP2C19, CYP2D6, or CYP2E1 (less than 0.01 pmol/min/pmol CYP). The formation rates of ISZ in CYP3A4 and CYP3A5 were 34.9 ± 1.4 and 15.1 ± 1.2 pmol per min/pmol P450, respectively. These results indicated that CYP3A4 and CYP3A5 both contribute to DS in HLMs, with CYP3A5 being metabolically less active than CYP3A4.

Recombinant human CYP isoforms were also employed to identify P450 isoforms involved in the subsequent metabolism of ISZ in human. After incubation at 37°C for 40 min,

DMD Fast Forward. Published on October 16, 2013 as DOI: 10.1124/dmd.113.053884
This article has not been copyedited and formatted. The final version may differ from this version.

four demethylated metabolites (M-1, M-2, M-3, and M-4) of ISZ were found in CYP3A4 and CYP3A5 (Supplemental Figure 2). While, no metabolites were observed in the incubations with CYP1A2, CYP2A6, CYP2B6, CYP2C8, CYP2C9, CYP2C19, CYP2D6, or CYP2E1 (less than 0.01 pmol/min/pmol CYP).

Correlation study. For DS hydroxylation to ISZ, a strong correlation was observed with a CYP3A marker, testosterone 6β-hydroxylation (r^2=0.85, $p<0.001$). DS hydroxylation also correlated with other CYP3A markers, such as, phenacetin O-deethylation (CYP1A2, r^2=0.31), coumarin 7-hydroxylation (CYP2A6, r^2=0.52), paclitaxel 6α-hydroxylation (CYP2C8, r^2=0.65), diclofenac 4'-hydroxylation (CYP2C9, r^2=0.05), S-Mephenytoin 4'-hydroxylation (CYP2C19, r^2=0.11), dextromethorphan O-demethylation (CYP2D6, r^2=0.31), and chlorzoxazone 6-hydroxylation (CYP2E1, r^2=0.29). The recombinant CYP1A2, CYP2A6, and CYP2C8 failed to metabolize DS (Figure 3). Therefore, CYP3A was the major CYP isoform involved in the formation of ISZ in HLM.

Kinetic study of DS. The kinetic parameters of ISZ formation in HLM, RLM and recombinant CYPs were determined. The formation rate of ISZ was linear up to 0.05 mg/ml and 0.2 mg/ml microsomal protein and in HLM and RLM for 10 min incubation, respectively. DS (0.2~50μM) was incubated with pooled HLM, RLM, recombinant CYP3A4, or recombinant CYP3A5. In parallel, TST (5~300μM), NIF (2~200μM) and MDZ (0.5~500μM) were also treated in the same incubation system. Over the whole concentration range tested, sigmoidal kinetics and substrate inhibition kinetics were observed for TST 6β-hydroxylation and MDZ 1'- hydroxylation, respectively, in accordance with the previous reports (Houston and Kenworthy, 2000). NIF oxidation was observed to obey the Michaelis-Menten kinetics

DMD Fast Forward. Published on October 16, 2013 as DOI: 10.1124/dmd.113.053884
This article has not been copyedited and formatted. The final version may differ from this version.

even though both sigmoidal and convex curves were reported for this substrate (Houston and Kenworthy, 2000). Importantly, DS C7-hydroxylation followed Michaelis-Menten kinetics, as depicted by linear Eadie-Hofstee plots in HLM, RLM and recombinant CYPs (Figure 4). By comparing the kinetic parameters (Table 2), DS showed higher affinity to CYP3A and metabolic capacity than that of TST, NIF and MDZ in HLM and RLM. V_{max} of DS 7-hydroxylation by CYP3A4 was nearly 2.5-fold higher than that by CYP3A5, while DS had similar binding affinity to both enzymes (K_m values of 3.2 and 4.1 μM, respectively), and yielded 3-fold clearance difference. Similar trends were also observed for TST and NIF, but the 1'-OH-MDZ formation rate in CYP3A4 was almost 6-fold lower than that in CYP3A5. Moreover, the intrinsic clearance of DS by CYP3A2 was nearly 2.5-fold higher than that by CYP3A1 (Supplemental Table 2 and Supplemental Figure 3).

Kinetic study of ISZ. In the same fashion as the DS kinetic study, the kinetic parameters of demethylated ISZ production in HLM and RLM were determined. The formation rates of demethylated metabolites were linear up to 0.4 mg/ml microsomal protein and in HLM and RLM for 30 min incubation, ISZ (5~300 μM) was incubated with the pooled HLM or RLM. In the range of concentrations tested, ISZ demethylation in liver microsomes complied with Michaelis-Menten kinetics, as evidenced by linear Eadie-Hofstee plot (Figure 5). It is noteworthy that DS exhibited 20~50 times higher affinity to CYP3A in HLM than ISZ did (Table 3 and Supplemental Table 3). Also, due to the low affinity of ISZ to CYP3A, the total intrinsic clearance (CL_{int}) of ISZ via demethylation only accounts for less than 5% of DS hydroxylation clearance in both HLM and RLM individually. Based on the above results, the proposed primary metabolic pathways of DS in HLM and RLM are shown in Figure 6.

Interaction Studies. In table 3, the interaction studies of DS in the presence of the three CYP3A substrates (MDZ, TST, and NIF) are demonstrated. The best model was selected mainly based on the criteria described as r^2 values and parameter S.D. estimates (Supplemental Table 4) Dixon and Lineweaver-Burk plots here show that inhibitions of DS by both TST and MDZ were best fitted to the mix inhibition type models, where inhibition kinetic parameter (K_i) in inhibiting CYP3A4 activity was calculated to be 74.1 ± 10.1 μM for TST and 6.6 ± 1.3 μM for MDZ. The α values yielded were 5.8 for TST and 3.8 for MDZ. Also, inhibitions of DS by TST and MDZ in CYP3A5 were both best fitted to competitive inhibition model with K_i values of 40.2 ±8.9 μM and 14.5 ± 3.3 μM, respectively. The inhibition of TST by DS was fitted to two-site kinetic model for sigmoidal kinetics, yielding a larger K_i value of 21.1 ± 3.3 μM in CYP3A4 than the K_i value of 16.3 ± 1.3 μM in CYP3A5. Here, affinity interaction factor, δ, yielded low values altogether with 0.73 in CYP3A4 and 0.58 in CYP3A5. The inhibition of MDZ by DS was fitted to two-site kinetic model for substrate inhibition kinetics, yielding K_i values of 17.3 ± 2.2 μM in CYP3A4 and 10.4 ± 1.8 μM in CYP3A5, and yielding low affinity interaction factor, δ, values of 0.26 in CYP3A4 and 0.41 in CYP3A5.

In contrast, Dixon and Lineweaver-Burk plots show that inhibition of DS by NIF was best fitted to noncompetitive inhibition model (Supplemental Figure 4), where its inhibition kinetic parameter (K_i) was calculated to be 24.8 ± 2.1 μM and 27.8 ± 4.2 μM for CYP3A4 and CYP3A5, respectively. Also, DS showed negligible inhibitory effects on NIF oxidation in both CYP3A4 and CYP3A5 (Supplemental Figure 5).

Discussion

In the present study, we identify that C-7- hydroxylation of DS is high-selectively catalyzed by CYP3A in liver microsomes from human and rat. DS hydroxylation was proved to obey Michaelis-Menten kinetics both in HLM, RLM and recombinant enzymes. For rat, the most commonly used animal species for pharmacokinetic studies, CYP3A1 and CYP3A2 predominantly catalyzed DS hydroxylation (Supplemental Figure 3). The similarities observed in metabolite profiles and kinetic properties between rat and human suggest that rat is a suitable surrogate animal model for further preclinical pharmacokinetic studies for DS. Primary results indicated mouse, pig and rabbit also showed similar metabolic profiles *in vitro*, which implied these species may be involved in further *in vivo* studies.

To date, it is known that most of CYP-catalyzed reactions can be described using the Michaelis-Menten equation, and the existing mathematical models used for the prediction of DDI or clearance are all based on Michaelis-Menten kinetic (Ito et al., 1998). Therefore, probe substrate with Michaelis-Menten kinetic was considered to be a “pragmatic” substrate. In the case of substrates with non-Michaelis-Menten kinetic, two or more molecules of substrates can simultaneously occupy the active site cavity and the kinetic parameters change with substrate occupancy. As a result, more complex mechanistic analyses are demanded; otherwise, false positive or negative prediction of DDI will result from classical Michaelis-Menten analysis. However, the most commonly used substrates of CYP3A recommended by FDA (http://www.fda.gov/Drugs/DevelopmentApprovalProcess/DevelopmentResources/DrugInteractionsLabeling/ucm093664.htm) do not obey the classical Michaelis-Menten kinetics, e.g.,

TST (Kenworthy et al., 2001), MDZ, NIF (Houston and Kenworthy, 2000), triazolam (Hallifax et al., 2005) and dextromethorphan (Witherow and Houston, 1999). Regardless of complex mechanism of non-Michaelis-Menten kinetics, ignoring it and truncating the data can lead to erroneous estimates of kinetic parameters (Lin et al., 2001). For example, TST was used in nearly 50% reported screening studies for DDI potentials (Yuan et al., 2002), but due to its atypical kinetic, its result is difficult to extrapolate to an *in vivo* setting (Foti et al., 2010). Thus, it is vital to find the substrate with classical Michaelis-Menten kinetic which can serve as an ideal probe for CYP3A activity.

The metabolite ISZ is a naturally occurring (+)-enantiomer of schizandrin. The asymmetric carbon at position 7 yields Z(*cis*)-(+)-schizandrin (7R, 8R) and E(*trans*)-(+)-isoschizandrin (7S, 8R). These *cis*- and *trans*-lignans possess similar biological properties, and the pharmacological activity resides mainly at the C7-hydroxyl (Ikeya et al., 1988; Warshawsky and Meyers, 1990). Then, the further metabolism of ISZ in microsomes and recombinant CYPs was also investigated. Demethylation was identified as the major metabolic pathway of ISZ where CYP3A4 and CYP3A5 were involved in this transformation indicated by the recombinant CYPs assays. It was almost unrealistic to biosynthesize and purify these demethylated metabolites for structure elucidation, because the metabolite formation rate was close to the limits of quantification. In comparison of the Michaelis-Menten kinetic profiles in HLM, both V_{max} and V_{max}/K_m values for schizandrin hydroxylation were 5 to 9-fold and at least 40% larger, respectively, than those for ISZ demethylation (Cao et al., 2010). This hints that the metabolic stability improves when Z (*cis*)-(+)-schizandrin is transformed into E (*trans*)-(+)-ISZ. Analysis of the

DMD Fast Forward. Published on October 16, 2013 as DOI: 10.1124/dmd.113.053884
This article has not been copyedited and formatted. The final version may differ from this version.

structure-metabolism relationship for the three lignans isolated from *Fructus Schisandrae*, suggests that the dibenzocyclooctadiene lignans with six methoxy groups on two benzene rings, is the most potent CYP3A substrate. This is observed through its single-site kinetic property, where hydroxylation or demethylation occurs either of C7 or C8, such as DS, ISZ and schizandrin (Cao et al., 2010). However, the lignans are prone to be CYP3A inhibitors when the methoxyl groups on phenyl are replaced with methylenedioxy ring (Iwata et al., 2004).

Notably, the subsequent ISZ demethylations was not observed when DS was incubated with HLM even at a very high substrate concentration (DS, 100 μM) within the linear reaction time range (data not shown). These data implied that the subsequent metabolism of ISZ might be abolished when DS was incubated with HLMs and RLM. This can be explained by the fact that DS exhibited 20 to 50-fold higher affinity to CYP3A in HLMs than ISZ did. Another explanation is the extremely low total CL_{int} of ISZ, which accounts for even less than 5% of DS hydroxylation clearance in HLM (Figure 6). The third is the fact that the logD values for DS and ISZ are calculated to 4.7 and 3.39, respectively (ChemAxon), which suggested that ISZ is a poor substrate compared with DS, owing to a change in lipophilicity driven by the introduction of a hydroxyl group. And one predominant metabolite was detected in the rat liver perfusate that mimics the *in vivo* situation. Furthermore, when incubated with either DS or ISZ in HLM or S9 fraction, no subsequent conjugates of ISZ or DS were observed in the UDPGA-, PAPS- or SAM-generating system. Observations here together suggest that DS was metabolized to a single metabolite, ISZ, via CYP3A with high selectivity. The existence of single catalytic/metabolic site for the probe could potentially

DMD Fast Forward. Published on October 16, 2013 as DOI: 10.1124/dmd.113.053884
This article has not been copyedited and formatted. The final version may differ from this version.

decrease the chance of erroneous judgment on prediction of DDI potentials, because the CYP modifiers might play seesaw effects on each metabolic site. Quinidine, a CYP3A4 substrate, can be metabolized to two or more metabolites, 3-hydroxyquinidine and quinidine N-oxide, despite exhibiting with Michaelis-Menten kinetic (Nielsen et al., 1999). MDZ can also metabolized to at least two metabolites, 1′-hydroxymidazolam and 4-hydroxymidazolam, modulators could exert different effects on each metabolite formation (Xia et al., 2009; Dong et al., 2011). As reported, erlotinib and panaxytriol, an active component in *Shenmai* injection (Zeng et al., 2013), both showed significant activation on MDZ 1′-hydroxylation, whereas the activation but not inhibition made it difficult for the *in vivo* extrapolation. Moreover，either glucuronidation of hydroxylmidazolam or direct glucuronidation of MDZ occurs *in vitro* and *in vivo* (Klieber et al., 2008; Hyland et al., 2009; Seo et al., 2010). The multiple metabolic pathways may partly compensate the decrease in MDZ metabolic clearance caused by the addition of the inhibitor and would also make it difficult for the *in vivo* quantification. Thus, the *in vivo* DDI prediction from the *in vitro* data for MDZ is lack of rationality at least in theory, despite the reported wealth of *in vitro* CYP3A inhibition data using MDZ and *in vivo* DDI data for MDZ.

On the other hand, using *in vitro* DDI studies as screening tools to evaluate the potential DDI *in vivo*, is based on the assumption that the drugs being analyzed are competing for the same enzyme catalytic site. (Wang et al., 2000). Thus, substrate interaction studies were conducted, where DS substrate substitution was analyzed in the presence of the three substrates of CYP3A. The kinetics of DS in CYP3A4 were best fitted to mix inhibition models resulting from competition, which yielded large α values of 5.8 and 3.8 in the

presence of TST and MDZ, respectively (Copeland, 2000); DS also exhibited competitive inhibition type in CYP3A5. DS markedly decreased the affinity for TST by CYP3A and TST-CYP3A complex, where low δ values of 0.73 and 0.58 were observed for CYP3A4 and CYP3A5, respectively, and low δ value suggested the affinity of inhibitor to the enzyme (or enzyme-substrate complex) increased but the affinity of substrate to the enzyme decreased. Also, similar inhibitory potencies of DS in CYP3A4 and CYP3A5 were evident in binding affinity for MDZ, where low δ values of 0.26 and 0.41 were observed for CYP3A4 and CYP3A5, respectively.

However, inhibition study using NIF showed different inhibition results. NIF noncompetitively inhibited DS hydroxylation in both CYP3A4 and CYP3A5. Moreover, DS was negligible in inhibiting NIF oxidation in both CYP3A4 and CYP3A5, even at high DS concentrations of up to 100 μM. Similar to the previous findings reported by Wang *et al* on the TST-NIF interaction (Wang et al., 2000), the unusual DS-NIF interaction seen in this study could be also explained by assuming that NIF has more freedom of movement and that it can bind to multiple metabolic sites, including the active site of CYP3A4/5 that DS binds and is fixed to. Consequently, NIF can inhibit the hydroxylation of DS, but the inhibition of NIF oxidation by DS cannot be demonstrated kinetically. Regardless of the possible mechanisms, the results in these inhibition studies reveal a complex interaction between NIF and CYP3A even though Michaelis-Menten kinetics was observed.

Overall, an assumption that the preferential binding domain of CYP3A is large, to which DS binds, can be inferred by its high affinity to the CYP3A active sites and the fact that DS competes strongly with both MDZ and TST for the mutual binding site. Furthermore, during

the drug-candidate screening and development process, *in vitro* pre-classification for a new drug can be recommended here by evaluating different types of kinetic profiles and by studying the similarity between binding regions of the investigational drug and of probe substrate. This can be then followed by predicting the possible doses to modify CYP activities for *in vivo* DDI risk assessment.

Here in this study, hydroxylation of DS at C-7 site to produce a single metabolite, ISZ, via CYP3A metabolism is shown as the exclusive metabolic pathway in human liver microsomes. Additionally, the kinetics profile obeyed the Michaelis-Menten kinetics. More importantly, DS is shown to compete with both TST and MDZ for a mutual binding site. And thus, DS is considered to be a good representative of MDZ and TST substrate subgroups. Thus, DS attributes to having the three criteria for a pragmatic *in vitro* probe: high-selectivity for CYP3A with a single metabolite, Michaelis-Menten kinetic property, and a broad range of substrate substitutions. Conclusively, DS serves as an ideal candidate for a novel and specific CYP3A probe substrate that can predict the modifications in CYP3A-derived metabolism.

Acknowledgments

We acknowledge the assistance of Dr. Di Hu for the analysis of NMR data.

Authorship Contributions

Participated in research design: Jingjing Wu, Yunfeng Cao, Yanyan Zhang, James Y. Hong, Liangliang Zhu, Guangbo Ge, Yong Liu, and Ling Yang.

Conducted experiments: Jingjing Wu, Yunfeng Cao, and Yanyan Zhang.

Performed data analysis: Jingjing Wu, Yunfeng Cao, Yanyan Zhang, James Y. Hong, Liangliang Zhu, Guangbo Ge, Yong Liu, and Ling Yang.

Wrote or contributed to the writing of the manuscript: Jingjing Wu, Yunfeng Cao, Yanyan Zhang, James Y. Hong, and Yong Liu.

Reference

Bjornsson TD, Callaghan JT, Einolf HJ, Fischer V, Gan L, Grimm S, Kao J, King SP, Miwa G, Ni L, Kumar G, McLeod J, Obach SR, Roberts S, Roe A, Shah A, Snikeris F, Sullivan JT, Tweedie D, Vega JM, Walsh J, and Wrighton SA (2003) The conduct of in vitro and in vivo drug-drug interaction studies: A PhRMA perspective. *J Clin Pharmacol* **43:**443-469.

Cao YF, Zhang YY, Li J, Ge GB, Hu D, Liu HX, Huang T, Wang YC, Fang ZZ, Sun DX, Huo H, Yin J, and Yang L (2010) CYP3A catalyses schizandrin biotransformation in human, minipig and rat liver microsomes. *Xenobiotica* **40:**38-47.

Copeland RA (2000) Enzymes: A Practical Introduction to Structure, Mechanism, and Data Analysis. *Wiley-VCH, New York.*

Dong PP, Fang ZZ, Zhang YY, Ge GB, Mao YX, Zhu LL, Qu YQ, Li W, Wang LM, Liu CX, and Yang L (2011) Substrate-dependent modulation of the catalytic activity of CYP3A by erlotinib. *Acta Pharmacol Sin* **32:**399-407.

Eagling VA, Tjia JF, Back DJ (1998) Differential selectivity of cytochrome P450 inhibitors against probe substrates in human and rat liver microsomes. *Br J Clin Pharmacol* **45**:107-114.

Emoto C, Murase S, Sawada Y, Jones BC, and Iwasaki K (2003) In vitro inhibitory effect of 1-aminobenzotriazole on drug oxidations catalyzed by human cytochrome P450 enzymes: a comparison with SKF-525A and ketoconazole. *Drug Metab Pharmacokinet* **18:**287-295.

Foti RS, Rock DA, Wienkers LC, and Wahlstrom JL (2010) Selection of Alternative CYP3A4 Probe Substrates for Clinical Drug Interaction Studies Using In Vitro Data and In

Vivo Simulation. *Drug Metab Dispos* **38:**981-987.

Frye RE (2004) Probing the world of cytochrone P450 enzymes. *Mol Interv* **4:**157-162.

Galetin A, Clarke SE, and Houston JB (2003) Multisite kinetic analysis of interactions between prototypical CYP3A4 subgroup substrates: Midazolam, testosterone, and nifedipine. *Drug Metab Dispos* **31:**1108-1116.

Galetin A, Ito K, Hallifax D, and Houston JB (2005) CYP3A4 substrate selection and substitution in the prediction of potential drug-drug interactions. *Journal of Pharmacology and Experimental Therapeutics* **314:**180-190.

Hallifax D, Rawden HC, Hakooz N, and Houston JB (2005) Prediction of metabolic clearance using cryopreserved human hepatocytes: kinetic characteristics for five benzodiazepines. *Drug Metab Dispos* **33:**1852-1858.

Houston JB and Kenworthy KE (2000) In vitro-in vivo scaling of CYP kinetic data not consistent with the classical Michaelis-Menten model. *Drug Metab Dispos* **28:**246-254.

Hyland R, Osborne T, Payne A, Kempshall S, Logan YR, Ezzeddine K, and Jones B (2009) In vitro and in vivo glucuronidation of midazolam in humans. *Brit J Clin Pharmaco* **67:**445-454.

Ikeya Y, Sugama K, Okada M, and Mitsuhashi H (1991) The Constituents of Schisandra Species .17. 2 Lignans from Schisandra-Sphenanthera. *Phytochemistry* **30:**975-980.

Ikeya Y, Taguchi H, Mitsuhashi H, Takeda S, Kase Y, and Aburada M (1988) The Constituents of Schizandra Chinensis .14. A Lignan from Schizandra Chinensis. *Phytochemistry* **27:**569-573.

Ito K, Iwatsubo T, Kanamitsu S, Ueda K, Suzuki H, and Sugiyama Y (1998) Prediction of pharmacokinetic alterations caused by drug-drug interactions: Metabolic interaction in the liver. *Pharmacol Rev* **50:**387-411.

Iwata H, Tezuka Y, Kadota S, Hiratsuka A, and Watabe T (2004) Identification and characterization of potent CYP3A4 inhibitors in Schisandra fruit extract. *Drug Metab Dispos* **32:**1351-1358.

Kalgutkar AS, Obach RS, and Maurer TS (2007) Mechanism-based inactivation of cytochrome P450 enzymes: Chemical mechanisms, structure-activity relationships and relationship to clinical drug-drug interactions and idiosyncratic adverse drug reactions. *Curr Drug Metab* **8:**407-447.

Kenworthy KE, Bloomer JC, Clarke SE, and Houston JB (1999) CYP3A4 drug interactions: correlation of 10 in vitro probe substrates. *Brit J Clin Pharmaco* **48:**716-727.

Kenworthy KE, Clarke SE, Andrews J, and Houston JB (2001) Multisite kinetic models for CYP3A4: Simultaneous activation and inhibition of diazepam and testosterone metabolism. *Drug Metab Dispos* **29:**1644-1651.

Klieber S, Hugla S, Ngo R, Arabeyre-Fabre C, Meunier V, Sadoun F, Fedeli O, Rival M, Bourrie M, Guillou F, Maurel P, and Fabre G (2008) Contribution of the N-glucuronidation pathway to the overall in vitro metabolic clearance of midazolam in humans. *Drug Metab Dispos* **36:**851-862.

Lin JH and Lu AYH (1997) Role of pharmacokinetics and metabolism in drug discovery and development. *Pharmacol Rev* **49:**403-449.

Lin Y, Lu P, Tang C, Mei Q, Sandig G, Rodrigues AD, Rushmore TH, and Shou M (2001)

Substrate inhibition kinetics for cytochrome P450-catalyzed reactions. *Drug Metab Dispos* **29:**368-374.

Liu HX, Hu Y, Liu Y, He YQ, Li W, and Yang L (2009) Hydroxylation of tanshinone IIa in human liver microsomes is specifically catalysed by cytochrome P4502A6. *Xenobiotica* **39:**382-390.

Liu KX, Kato Y, Kaku TI, Santa T, Imai K, Yagi A, Ishizu T, and Sugiyama Y (2000) Hydroxyprolylserine derivatives JBP923 and JBP485 exhibit the antihepatitis activities after gastrointestinal absorption in rats. *J Pharmacol Exp Ther* **294**:510-515

Liu Y, Ramirez J, House L, and Ratain MJ (2010) Comparison of the Drug-Drug Interactions Potential of Erlotinib and Gefitinib via Inhibition of UDP-Glucuronosyltransferases. *Drug Metab Dispos* **38:**32-39.

Lowry OH, Rosebrough NJ, Farr AL, and Randall RJ (1951) Protein Measurement with the Folin Phenol Reagent. *J Biol Chem* **193:**265-275.

Nielsen TL, Rasmussen BB, Flinois JP, Beaune P, and Brosen K (1999) In vitro metabolism of quinidine: The (3S)-3-hydroxylation of quinidine is a specific marker reaction for cytochrome P-4503A4 activity in human liver microsomes. *Journal of Pharmacology and Experimental Therapeutics* **289:**31-37.

Patki KC, von Moltke LL, and Greenblatt DJ (2003) In vitro metabolism of midazolam, triazolam, nifedipine, and testosterone by human liver microsomes and recombinant cytochromes P450: Role of CYP3A4 and CYP3A5. *Drug Metab Dispos* **31:**938-944.

Rae JM, Soukhova NV, Flockhart DA, and Desta Z (2002) Triethylenethiophosphoramide is a specific inhibitor of cytochrome P4502B6: Implications for cyclophosphamide

metabolism. *Drug Metab Dispos* **30:**525-530.

Seo K-A, Bae SK, Choi Y-K, Choi CS, Liu K-H, and Shin J-G (2010) Metabolism of 1 '- and 4-Hydroxymidazolam by Glucuronide Conjugation Is Largely Mediated by UDP-Glucuronosyltransferases 1A4, 2B4, and 2B7. *Drug Metab Dispos* **38:**2007-2013.

Stresser DM, Blanchard AP, Turner SD, Erve JCL, Dandeneau AA, Miller VP, and Crespi CL (2000) Substrate-dependent modulation of CYP3A4 catalytic activity: Analysis of 27 test compounds with four fluorometric substrates. *Drug Metab Dispos* **28:**1440-1448.

Turan VK, Mishin VM, Thomas PE (2001) Clotrimazole is a selective and potent inhibitor of rat cytochrome P450 3A subfamily-related testosterone metabolism. *Drug Metab Dispos* **29**:837-842.

Walsky RL, Obach RS, Gaman EA, Gleeson JPR, and Proctor WR (2005) Selective inhibition of human cytochrome P4502C8 by montelukast. *Drug Metab Dispos* **33:**413-418.

Wang RW, Newton DJ, Liu N, Atkins WM, and Lu AYH (2000) Human cytochrome P-450 3A4: In vitro drug-drug interaction patterns are substrate-dependent. *Drug Metab Dispos* **28:**360-366.

Warshawsky AM and Meyers AI (1990) Asymmetric Total Synthesis of Dibenzocyclooctadiene Lignans (-)-Schizandrin and (-)-Isoschizandrin - Structure Revision of (+)-Isoschizandrin. *J Am Chem Soc* **112:**8090-8099.

Wei H, Sun L, Tai Z, Gao S, Xu W, and Chen W (2010) A simple and sensitive HPLC method for the simultaneous determination of eight bioactive components and fingerprint

analysis of Schisandra sphenanthera. *Analytica chimica acta* **662:**97-104.

Wienkers LC and Heath TG (2005) Predicting in vivo drug interactions from in vitro drug discovery data. *Nat Rev Drug Discov* **4:**825-833.

Wille SMR, Cooreman SG, Neels HM, and Lambert WEE (2008) Relevant issues in the monitoring and the toxicology of antidepressants. *Crit Rev Cl Lab Sci* **45:**25-89.

Witherow LE and Houston JB (1999) Sigmoidal kinetics of CYP3A substrates: an approach for scaling dextromethorphan metabolism in hepatic microsomes and isolated hepatocytes to predict in vivo clearance in rat. *The Journal of pharmacology and experimental therapeutics* **290:**58-65.

Wu JJ, Ai CZ, Liu Y, Zhang YY, Jiang M, Fan XR, Lv AP, and Yang L (2012) Interactions between Phytochemicals from Traditional Chinese Medicines and Human Cytochrome P450 Enzymes. *Curr Drug Metab* **13:**599-614.

Xia CH, Sun JG, Wang GJ, Shang LL, Zhang XX, Zhang R, Wang XJ, Hao HP, and Xie L (2009) Differential effect of Shenmai injection, a herbal preparation, on the cytochrome P450 3A-mediated 1 '-hydroxylation and 4-hydroxylation of midazolam. *Chem-Biol Interact* **180:**440-448.

Yano JK, Wester MR, Schoch GA, Griffin KJ, Stout CD, and Johnson EF (2004) The structure of human microsomal cytochrome P450 3A4 determined by X-ray crystallography to 2.05-angstrom resolution. *J Biol Chem* **279:**38091-38094.

Yuan R, Madani S, Wei XX, Reynolds K, and Huang SM (2002) Evaluation of cytochrome P450 probe substrates commonly used by the pharmaceutical industry to study in vitro drug interactions. *Drug Metab Dispos* **30:**1311-1319.

Zeng CW, He F, Xia CH, Zhang H, and Xiong YQ (2013) Identification of the Active Components in Shenmai Injection that Differentially Affect Cyp3a4-Mediated 1 '-Hydroxylation and 4-Hydroxylation of Midazolam. *Drug Metab Dispos* **41:**785-790.

Zhou SF, Xue CC, Yu XQ, Li C, and Wang G (2007) Clinically important drug interactions potentially involving mechanism-based inhibition of cytochrome p450 3A4 and the role of therapeutic drug monitoring. *Ther Drug Monit* **29:**687-710.

Footnotes

This work was supported by the National Key Technology Major Project of China [Grants 2012ZX09506001-006 & 2012ZX10002011-008], and the National Natural Science Foundation of China [Grants 81202587, 81102507 & 81072698].

DMD Fast Forward. Published on October 16, 2013 as DOI: 10.1124/dmd.113.053884
This article has not been copyedited and formatted. The final version may differ from this version.

Legends for Figures

Figure 1. Representative UFLC profiles of DS, ISZ and their metabolites in human liver microsomes, rat liver microsomes, and rat liver perfusate. DS (50 μM) was incubated with liver microsomes (0.3 mg/ml) at 37°C for 20 min (A) from different species with NADPH-generating system; the recirculating perfusate was obtained after a bolus introduction of DS (50 μM) to the perfusate over 30 min. Meanwhile, ISZ (100 μM) was incubated with liver microsomes (0.4 mg/ml) at 37°C for 40 min from different species and schizandrin (100 μM) was incubated with human liver microsomes (0.3 mg/ml) at 37°C for 20 min with NADPH-generating system (B).

Figure 2. Effects of selective CYP inhibitors on the formation of metabolite ISZ (M) in human liver microsomes (A) and rat liver microsomes (B). Results are the mean ± S.D. from three experiments carried out in duplicate.

Figure 3. The formation of metabolite M (ISZ) catalyzed by various recombinant human CYPs. DS (50μM) was incubated with various recombinant human CYPs (40–80 nM) at 37°C for 20 min. Data represent the mean of three experiments carried out in duplicate.

Figure 4. Kinetic plots of DS metabolism after incubation with pooled human liver microsomes (A), pooled rat liver microsomes (B), recombinant CYP3A4 (C) and CYP3A5 (D). Eadie-Hofstee plots are shown for DS hydroxylation. Lines represent linear regressions of Eadie-Hofstee transformed data best-fits to a Michaelis-Menten model (A, B, C and D).

Figure 5. Kinetic plots of ISZ metabolism after incubation with pooled human liver microsomes (A) and pooled rat liver microsomes (B). Eadie-Hofstee plots are shown for both ISZ demethylation. Lines represent linear regressions of Eadie-Hofstee transformed data

best-fits to a Michaelis-Menten model (A and B).

Figure 6. The proposed primary metabolic pathways of DS in liver microsomes from human and rat.

Table 1. Proton and carbon NMR chemical shift assignments for deoxyschizandrin and its metabolite (M)

NO.	Deoxyschizandrin		M (isoschizandrin)			
	δ^1H	δ^{13}C	δ^1H	δ^{13}C	HMBC (H→C)	NOESY
1		151.5		151.3		
2		140.1		132.8		
3		152.8		151.9		
4	6.54 (s)	107.1	6.64 (s)	110.4	C-1, C-2, C-3, C-5, C-6, C-16	H-6, H-17
5		139.1		140.5		
	α: 2.55 (dd, J = 13.8, 7.8 Hz)		α: 2.68 (d, J = 13.2 Hz)			
6	β: 2.50 (dd, J = 13.8, 1.8 Hz)	35.6	β: 2.62 (d, J = 13.2 Hz)	48.2	C-4, C-5, C-7, C-8, C-16, C-17	H-4, H-8, H-17
7	1.81 (m)	40.7	1.83 (m)	47.9		
8	1.91 (m)	33.7	1.73 (m)	73.8	C-7, C-10, C-17, C-18	H-6, H-9, H-11, H-18
	α: 2.28 (dd, J = 13.2, 9.6 Hz)		α: 2.22 (m)			
9	β: 2.06 (br d, J = 13.2 Hz)	39.1	β: 2.18 (m)	37.1	C-7, C-8, C-10, C-11, C-15, C-18	H-8, H-11, H-18
10		133.9		140.1		
11	6.54 (s)	110.4	6.56 (s)	107.1	C-9, C-10, C-12, C-13, C-14, C-15	H-8, H-9

12		151.6		153.1		
13		139.7		138.1		
14		151.4		151.4		
15		123.3		121.7		
16		122.3		123.3		
17	1.00 (d, *J* = 7.2 Hz)	12.6	1.1 (d, *J* = 7.2 Hz)	18.9	C-6,C-7,C-8	H-4, H-6
18	0.74 (d, *J* = 6.6 Hz)	21.8	1.07 (s)	20.7	C-7,C-8	H-8, H-9
				61.0, 60.9,		
	3.59×2, 3.87, 3.88,3.89, 3.90	60.9×2, 60.5×2,	3.60×2, 3.87,3.89, 3.90	60.6×2,		
OMe	(each 3H, s)	55.9×2	×2 (each 3H, s)	55.9×2		

All spectra were recorded on a Bruker ARX-600 spectrometer, in $CDCl_3$; Abbreviations:br=broad, d=doublet, m=multiplet, s=singlet, J=coupling constant. HMBC, heteronuclear multiple-bond correlation spectroscopy; NOESY, nuclear Overhauser effect spectroscopy.

Table 2. Kinetic parameters of DS, NIF, TST metabolism in HLM, RLM, recombinant human CYP3A4 and CYP3A5

Enzyme source	DS			NIF			TST				MDZ			
	M (isoschizandrin)			OX-NIF			6β-HTS				1'-OH-MDZ			
	V_{max}	K_m	CL_{int}	V_{max}	K_m	CL_{int}	V_{max}	S_{50}	n	CL_{max} [a]	V_{max}	K_s	K_{si}	CL_{int}
HLM	623±9.9	1.6±0.1	389	4461±59	15.3±1.0	297	5484±90	53.1±5.1	1.4±0.1	56.8	119 ±4.6	3.5±0.4	228±43	33.7
RLM	168±2.4	1.4±0.3	120	1360±16	20.3±0.8	67.0	2563±78	61.2±4.0	1.2±0.1	26.7	96.9±3.8	6.1±1.7	206±41	16.1
CYP3A4	36.7±0.3	3.2±0.1	11.5	35.7±0.7	10.2±0.7	3.50	101±1.1	35.1±3.2	1.2±0.1	1.80	5.9±0.2	1.3±0.2	114±17	4.50
CYP3A5	16.1±2.4	4.1±0.1	3.90	18.4±0.3	15.8±0.8	1.20	44.7±1.3	89.5±5.2	1.3±0.1	0.29	34.2±2.5	4.1±0.8	173±52	8.30

K_m values were in μM; V_{max} values were in pmol/min/mg for liver microsomes, or in pmol/min/pmol CYP for CYP3A4; CL_{int} (V_{max}/K_m) values were in μl/mg/min for liver microsomes, or in μl/pmol/min for CYP3A4 & CYP3A5; a, TST clearance was obtained by V_{max}/K_m corrected with Hill coefficient (Houston and Kenworthy, 2000). Each value was the mean ± S.D. of three determinations performed in duplicate.

Table 3. Kinetic parameters for the *in vitro* inhibitory effects of pairs of CYP3A substrates in recombinant human CYP3A4 and CYP3A5

Substrates	Inhibitors	CYP3A4					CYP3A5			
		Model *	K_i (μM)	α	δ	Goodness of fit (R^2)	Model *	K_i (μM)	δ	Goodness of fit (R^2)
DS	NIF	eq. 2	24.8 ± 2.1	--	--	0.990	eq. 2	27.8 ± 4.2	--	0.968
	MDZ	eq. 3	6.6 ± 1.3	3.8 ± 0.8	--	0.994	eq. 1	14.5 ± 3.3	--	0.972
	TST	eq. 3	74.1 ± 10.1	5.8 ± 1.2	--	0.988	eq. 1	40.2 ± 8.9	--	0.977
NIF		eq. 1~5			N/A		eq. 1~5		N/A	
MDZ	DS	eq. 4	17.3 ± 2.2	--	0.26 ± 0.1	0.960	eq. 4	10.4 ± 1.8	0.41 ±0.2	0.988
TST		eq. 5	21.1 ± 3.3	--	0.73 ± 0.2	0.989	eq. 5	6.8 ± 1.3	0.89 ± 7.8	0.979

N/A: Not available; * Inhibitory kinetic models as described in "Materials and methods". Each value was the mean ± S.D. of three determinations performed in duplicate.

Figure 1

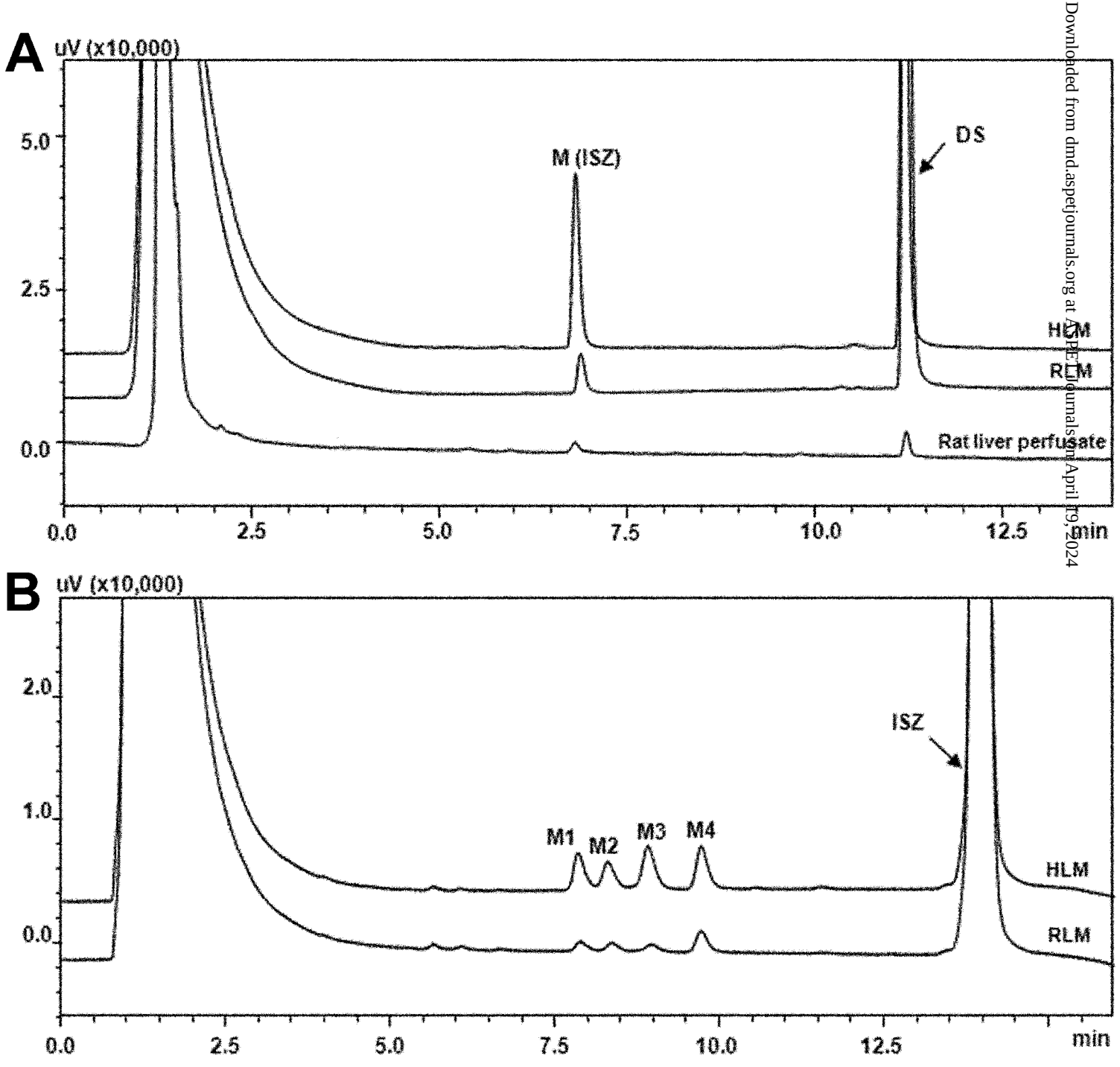

Figure 2

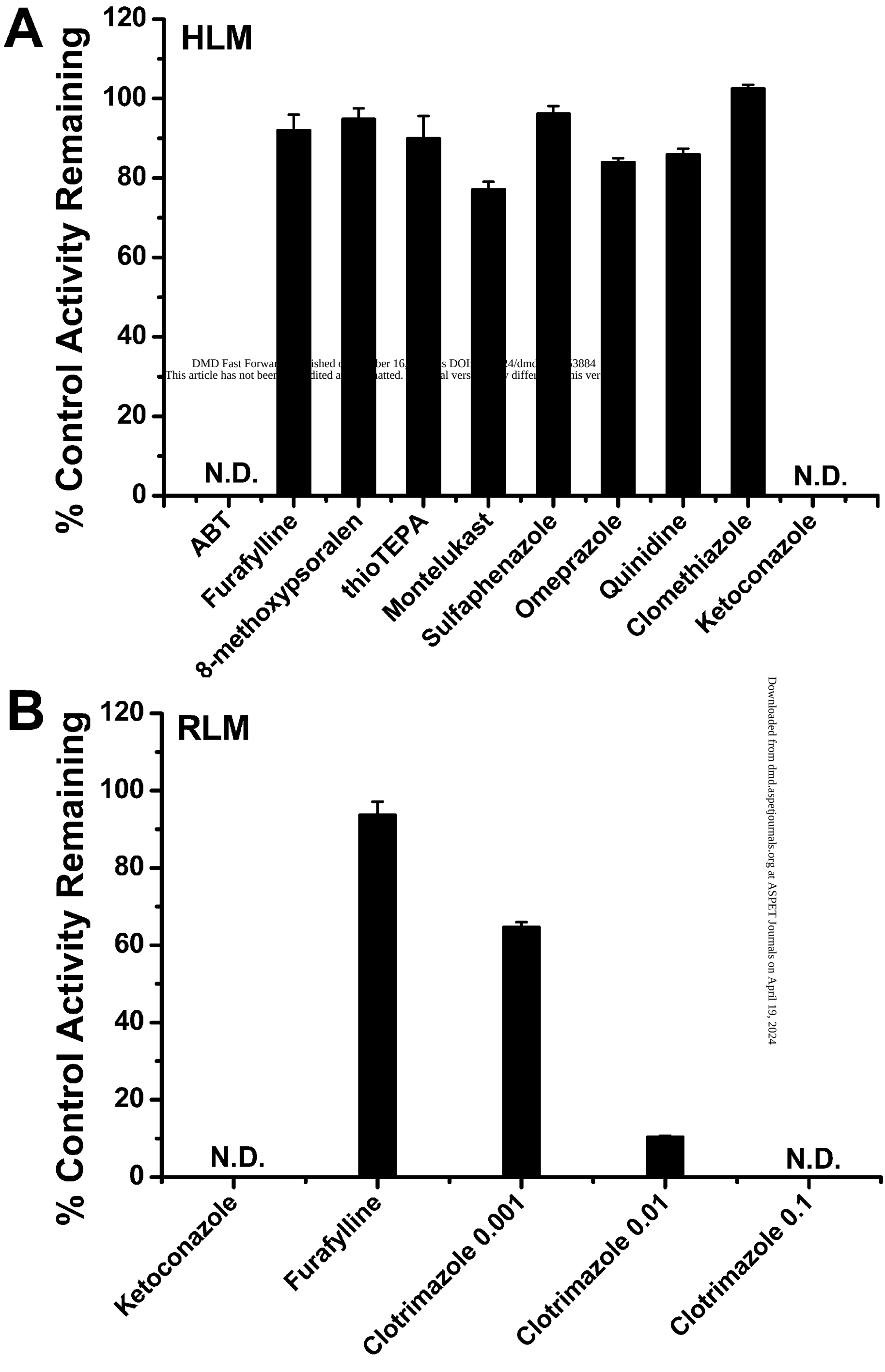

Figure 3

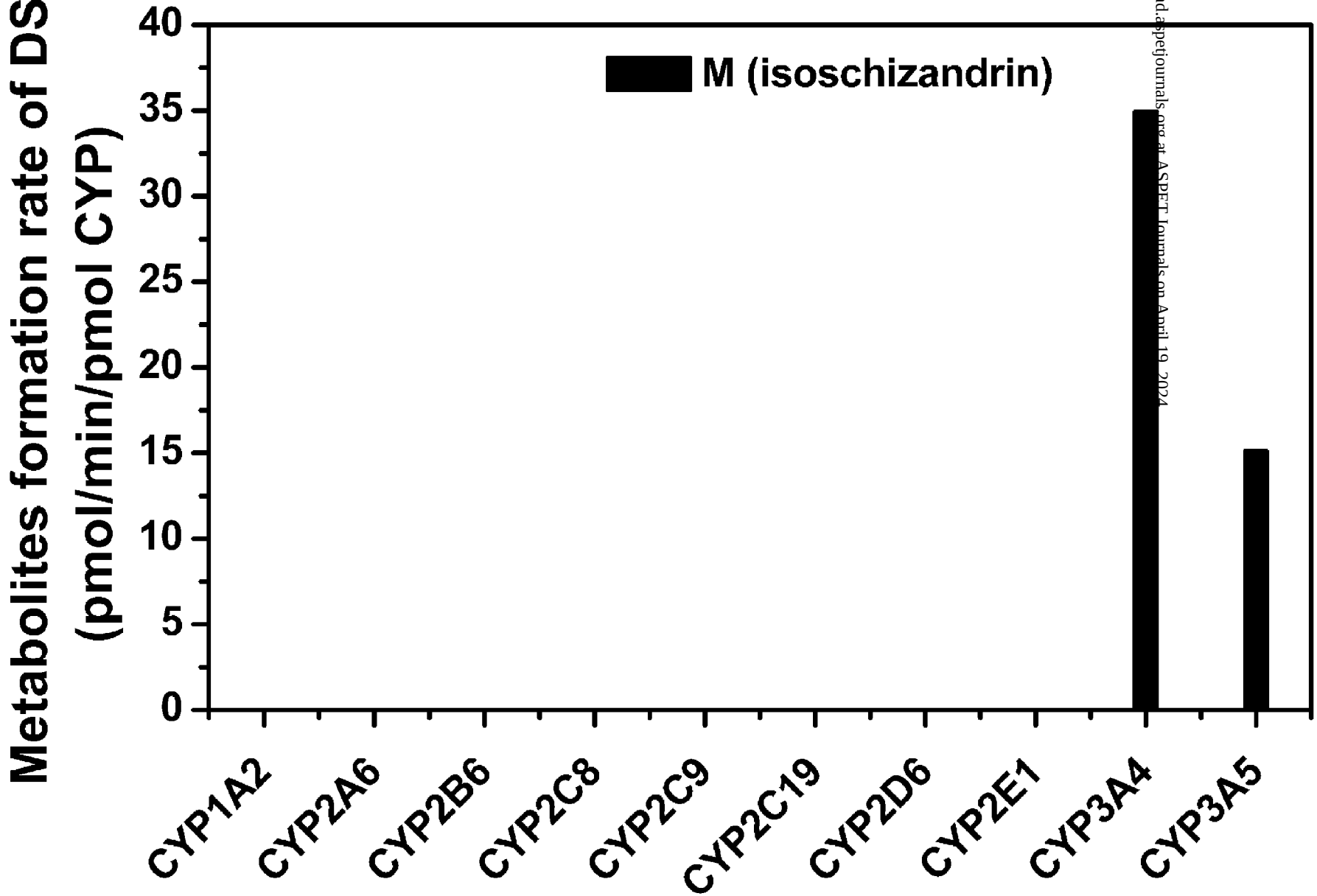

Figure 4

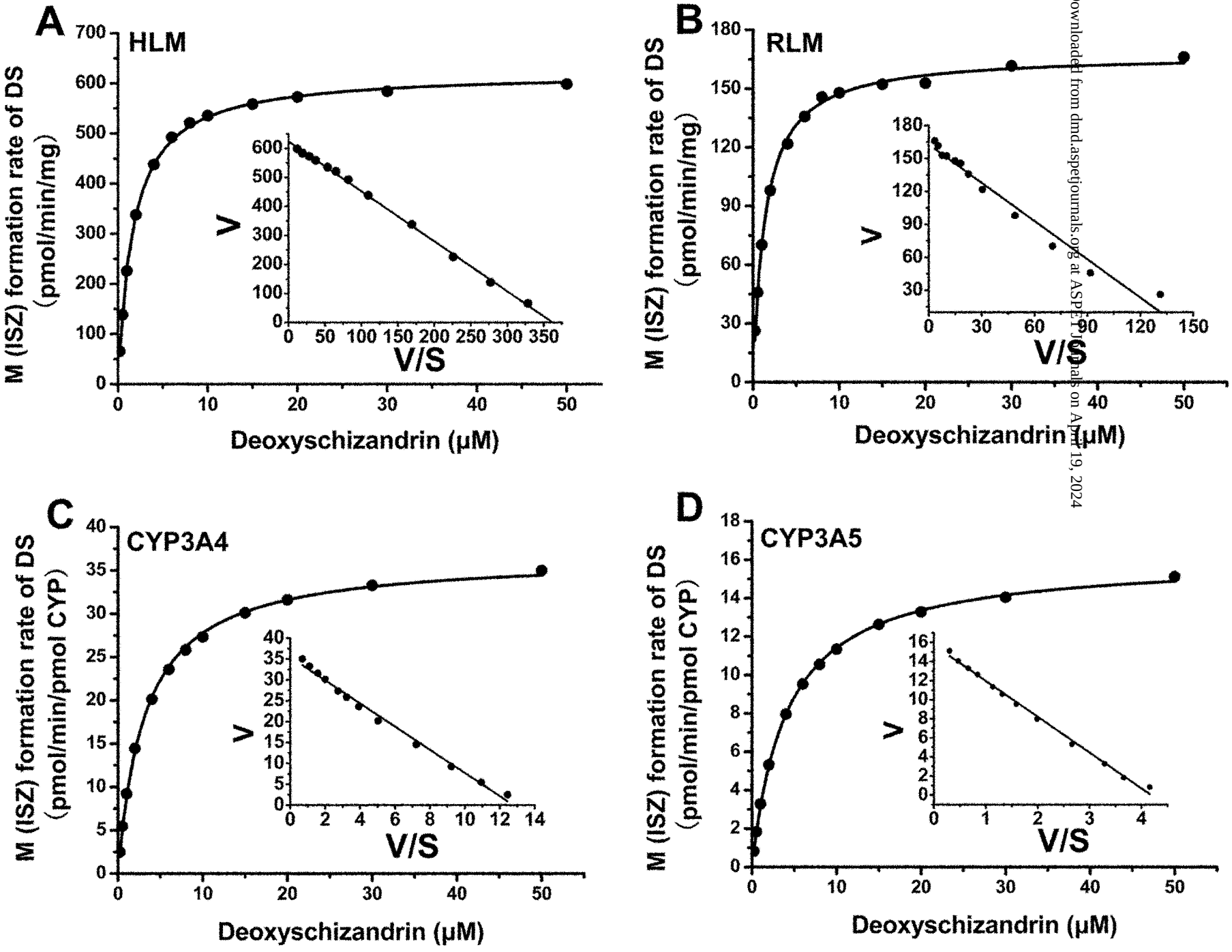

Figure 5

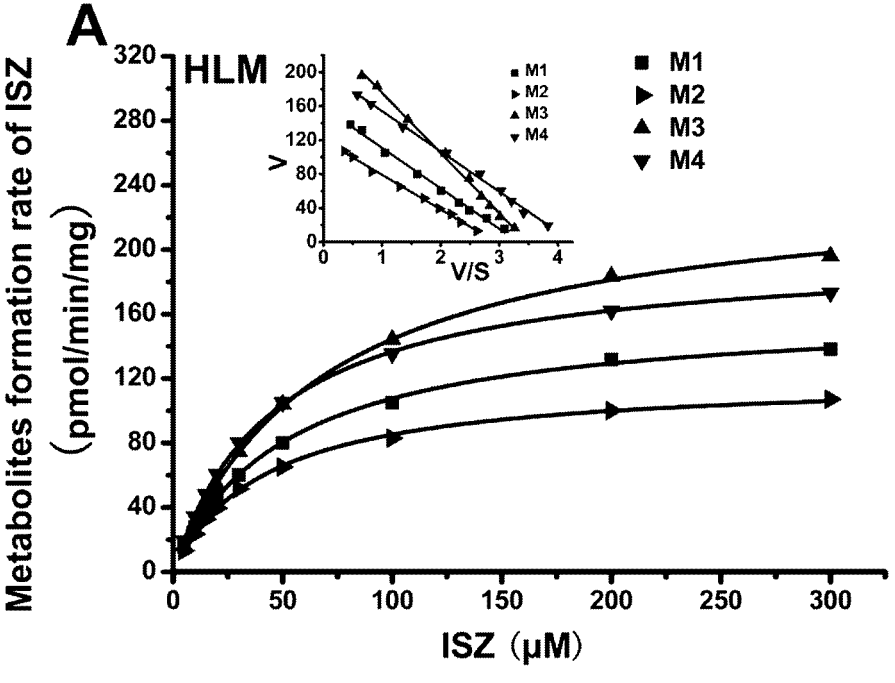

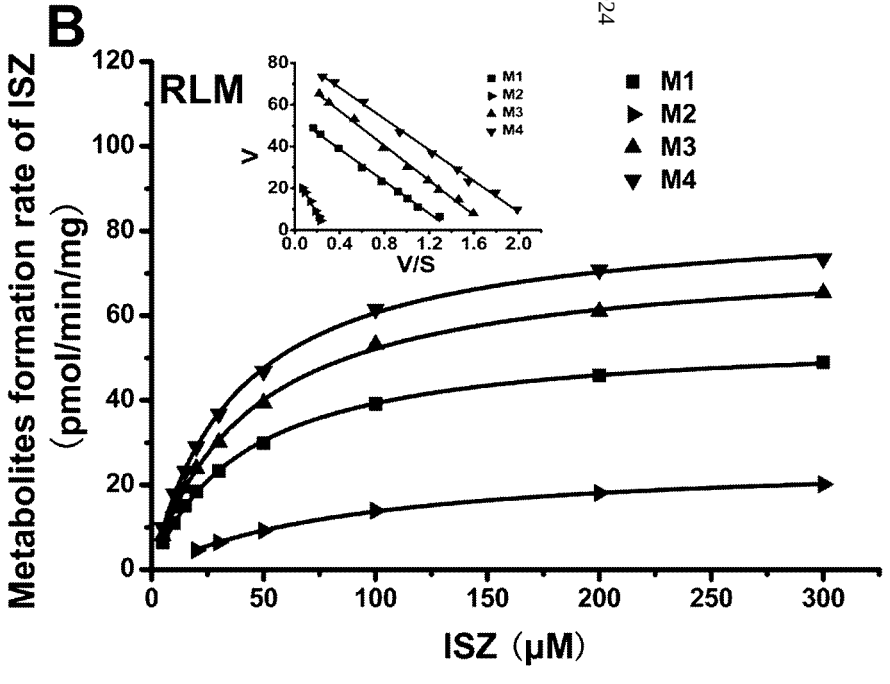

Figure 6

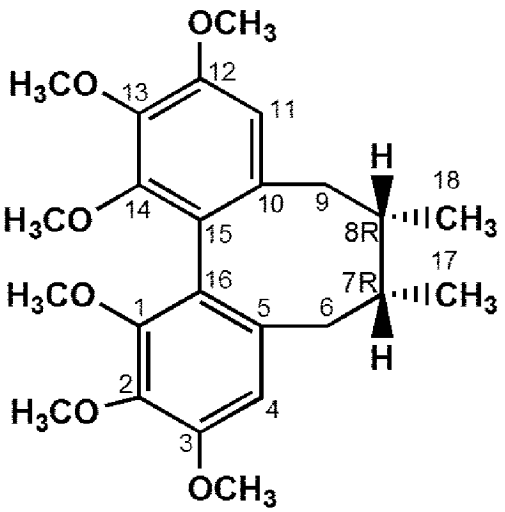

Deoxyschizandrin

CYP3A

HLM:
K_m=1.6 μM
CL_{int}=389 μl/min/mg

RLM:
K_m=1.4 μM
CL_{int}=120 μl/min/mg

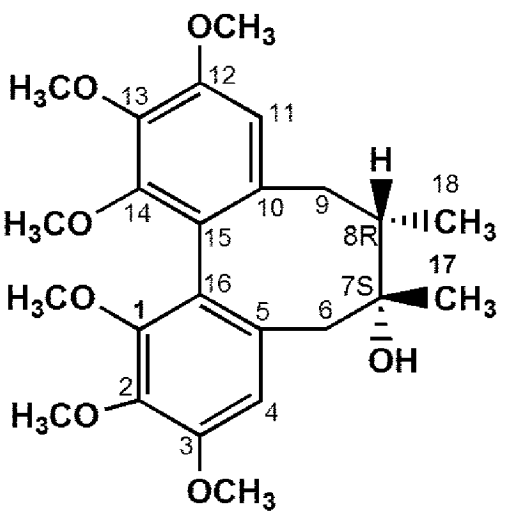

Isoschizandrin (M)

Phase II enzymes

Phase II enzymes

CYP3A

	HLM:	RLM:
M-1	K_m=45.1 μM CL_{int}=3.7 μl/min/mg	K_m=37.7 μM CL_{int}=1.5 μl/min/mg
M-2	K_m=36.5 μM CL_{int}=3.4 μl/min/mg	K_m=121.9 μM CL_{int}=0.2 μl/min/mg
M-3	K_m=75.9 μM CL_{int}=3.1 μl/min/mg	K_m=41.3 μM CL_{int}=1.8 μl/min/mg
M-4	K_m=48.5 μM CL_{int}=4.1 μl/min/mg	K_m=35.9 μM CL_{int}=2.4 μl/min/mg

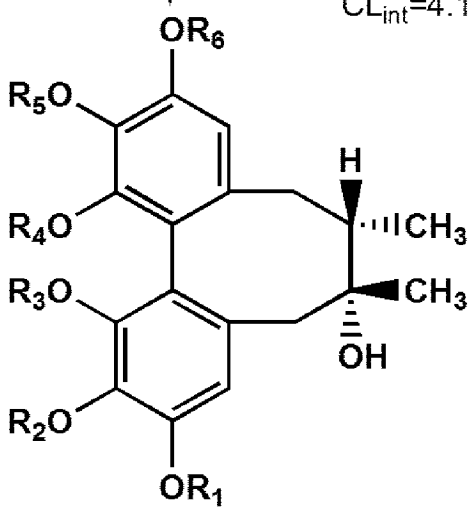

M1-4* : $R_{1\text{-}6}$ = CH_3 or H

* There is only one substituent is hydrogen.

Supplemental Data

Deoxyschizandrin, a Naturally Occurring Lignan, is a Specific probe Substrate of Human Cytochrome P450 3A

Jingjing Wu, Yunfeng Cao, Yanyan Zhang, Yong Liu, James Y. Hong, Liangliang Zhu, Guangbo Ge, Ling Yang

Laboratory of Pharmaceutical Resource Discovery, Dalian Institute of Chemical Physics, Chinese Academy of Sciences, 457 Zhongshan Road, Dalian, China (J.W., Y.C., Y.Z., Y.L., L.Z., G.G., L.Y.);

Department of Biopharmaceutical Sciences, University of Illinois, Chicago, USA (J.Y.H.);

Shanghai Institute of Planned Parenthood Research, Shanghai, 200032, China (Y.C.);

Graduate University of Chinese Academy of Sciences, Beijing, China (J.W., L.Z.)

Drug Metabolism and Disposition

Legends of supplemental Figures:

Figure 1. Representative UFLC profiles of DS and its metabolites in liver microsomes from human, mouse, pig and rabbit. DS (50 μM) was incubated with liver microsomes (0.3 mg/ml) at 37℃ for 20 min from different species with NADPH-generating system.

Figure 2. The formation of metabolite M-1, M-2, M-3 and M-4 catalyzed by various recombinant human CYPs. ISZ (100 μM) was incubated with various recombinant human CYPs (0.5 nM) at 37℃ for 40 min. Data represent the mean of duplicate incubations.

Figure 3. Kinetic plots of DS metabolism after incubation with recombinant rat CYP3A1 and CYP3A2. Eadie-Hofstee plots are shown for DS hydroxylation. Lines represent linear regressions of Eadie-Hofstee transformed data best-fits to a Michaelis-Menten model.

Figure 4. Reversible inhibition of DS hydroxylation by NIF in the recombinant human CYP3A4 and CYP3A5. A: Dixon plot of the inhibitory effect of NIF on DS hydroxylation activity in CYP3A4; B: Lineweaver-Burk plot of the inhibitory effect of NIF on DS hydroxylation activity in CYP3A4; C: Dixon plot of the inhibitory effect of NIF on DS hydroxylation activity in CYP3A5; D: Lineweaver-Burk plot of the inhibitory effect of NIF on DS hydroxylation activity in CYP3A5.

Figure 5. Inhibition of NIF oxidation by DS in the recombinant human CYP3A4 (A) and CYP3A5 (B).

Table 1. Retention times (t_R), molecular weights (M.W.) and MS data for metabolites of DS and ISZ in HLM

Lignans	t_R[a] (min)	Identification	M.W.[b]	Molecular ions (ESI^+, m/z)
M (isoschizandrin)	6.8	7- hydroxylation	432	471 $[M+K]^+$
M-1	7.8	Demethylation	418	457 $[M+K]^+$
M-2	8.2	Demethylation	418	457 $[M+K]^+$
M-3	8.8	Demethylation	418	457 $[M+K]^+$
M-4	9.7	Demethylation	418	457 $[M+K]^+$

[a] t_R, retention time on UFLC/UV; [b] MW, molecular weight

Table 2. **Kinetic parameters of DS metabolism in recombinant rat CYP3A1 and CYP3A2.**

	V_m	K_m	CL_{int}
CYP3A1	2.4 ±0.02	4.8 ±0.1	0.49
CYP3A2	12.6 ±0.12	10.4 ±0.25	1.22

K_m values were in μM; V_{max} values were in nmol/min/mg CYP; CL_{int} (V_{max}/K_m) values were in ml/min/mg CYP. The concentrations ranges of M (isoschizandrin) in HLM and RLM were both 0.2-50 μM. Each value was the mean ± S.D. of three determinations performed in duplicate.

Table 3. Kinetic parameters of M (isoschizandrin) metabolism in HLM and RLM

Species	M-1			M-2			M-3			M-4		
	V_{max}	K_m	CL_{int}	V_{max}	K_m	CL_{int}	V_{max}	K_m	CL_{int}	V_{max}	K_m	CL_{int}
Human	168±4.2	45.1±3.5	3.7	125±2.5	36.5±2.5	3.4	236±3.8	75.9±4.7	3.1	197±2.6	48.5±2.7	4.1
Rat	55.7±0.5	37.7±1.8	1.5	25.4±1.0	122±24	0.21	75.4±0.9	41.3±2.7	1.8	85.9±1.3	35.9±2.9	2.4

K_m values were in μM; V_{max} values were in pmol/min/mg for liver microsomes; CL_{int} (V_{max}/K_m) values were in μl/mg/min for liver microsomes. The concentrations ranges of M (isoschizandrin) in HLM and RLM were both 5-300 μM. Each value was the mean ± S.D. of three determinations performed in duplicate.

Table 4. **Comparison of the parameters generated with different models for the inhibitory effects of pairs of CYP3A substrates.**

Substrates	Inhibitors	CYP3A4			CYP3A5		
		Model	*K*i (μM)	Goodness of fit (R^2)	Model	*K*i (μM)	Goodness of fit (R^2)
DS	NIF	eq. 1	5.1 ± 1.2	0.972	eq. 1	7.3 ± 2.3	0.947
		eq. 2*	24.7 ± 2.1	0.990	eq. 2*	27.8 ± 4.2	0.968
		eq. 3	16.9 ± 6.0	0.990	eq. 3	31.4 ± 24.6	0.968
DS	MDZ	eq. 1	2.6 ± 0.4	0.984	eq. 1*	14.5 ± 3.3	0.972
		eq. 2	14.1 ± 1.1	0.991	eq. 2	94.4 ± 20.2	0.959
		eq. 3*	6.6 ± 1.3	0.994	eq. 3	17.85 ± 6.7	0.973
DS	TST	eq. 1	50.4 ± 8.2	0.986	eq. 1*	40.2 ± 8.9	0.977
		eq. 2	170.6 ± 20.5	0.984	eq. 2	258.2 ± 53.2	0.954
		eq. 3*	74.1 ± 10.1	0.988	eq. 3	42.2 ±15.0	0.977
MDZ	DS	eq. 1	5.3 ± 2.2	0.909	eq. 1	9.6 ± 1.8	0.981
		eq. 2	36.2 ± 8.6	0.921	eq. 2	37.7 ± 6.8	0.966
		eq. 3	13.4 ± 10.2	0.927	eq. 3	9.6 ± 5.1	0.981
		eq. 4*	17.3 ± 2.2	0.960	eq. 4*	10.4 ± 1.8	0.988
TST	DS	eq. 1	18.6 ± 3.3	0.978	eq. 1	9.1 ± 3.7	0.886
		eq. 2	53.9 ± 8.9	0.971	eq. 2	37.3 ± 10.6	0.887
		eq. 3	19.8 ± 7.0	0.978	eq. 3	15.6 ± 13.4	0.893
		eq. 5*	21.1 ± 3.3	0.989	eq. 5*	6.8 ± 1.3	0.979

* The best model that was selected using the criteria described (goodness of fit and parameter S.D. estimates).

Figure 1

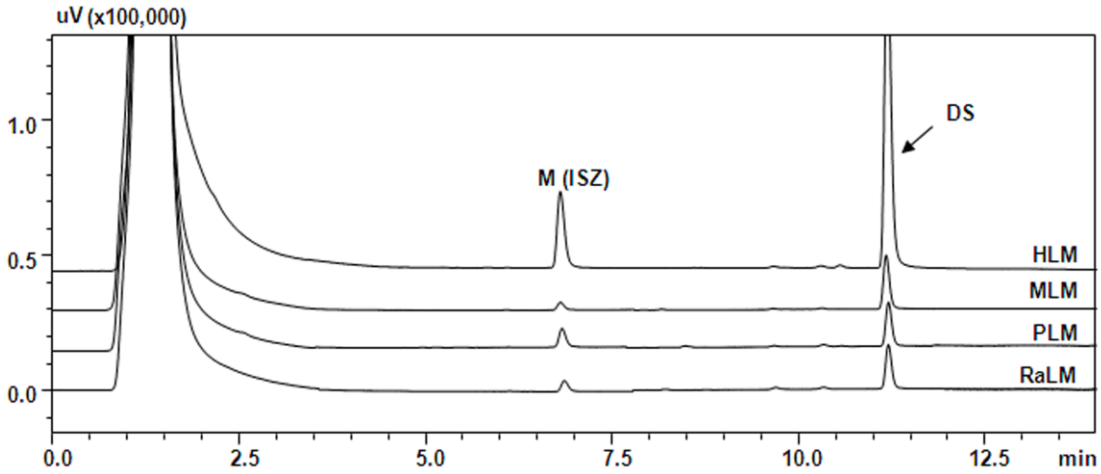
uV (x100,000)
1.0
0.5
0.0
M (ISZ)
DS
HLM
MLM
PLM
RaLM
0.0
2.5
5.0
7.5
10.0
12.5
min

Figure 2

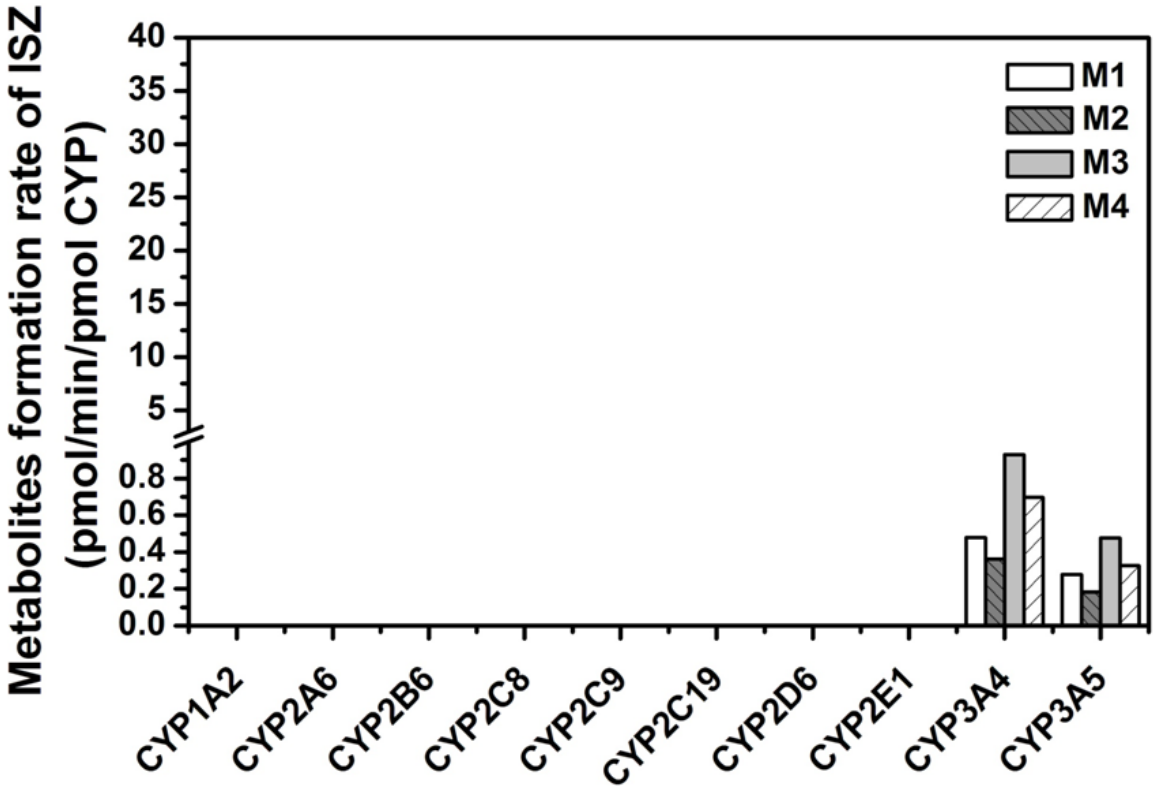
Metabolites formation rate of ISZ
(pmol/min/pmol CYP)
40
35
30
25
20
15
10
5
0.8
0.6
0.4
0.2
0.0
M1
M2
M3
M4
CYP1A2
CYP2A6
CYP2B6
CYP2C8
CYP2C9
CYP2C19
CYP2D6
CYP2E1
CYP3A4
CYP3A5

Figure 3

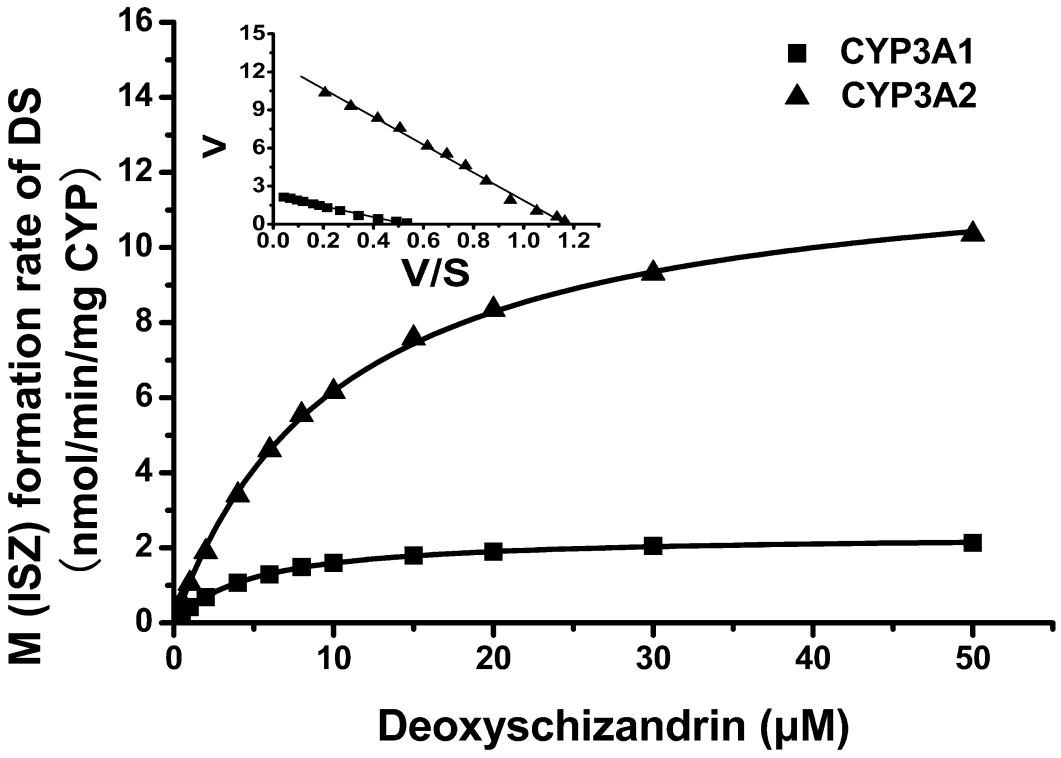
M (ISZ) formation rate of DS
(nmol/min/mg CYP)
Deoxyschizandrin (μM)
CYP3A1
CYP3A2
V
V/S
0
2
4
6
8
10
12
14
16
0
10
20
30
40
50
0
3
6
9
12
15
0.0
0.2
0.4
0.6
0.8
1.0
1.2

Figure 4

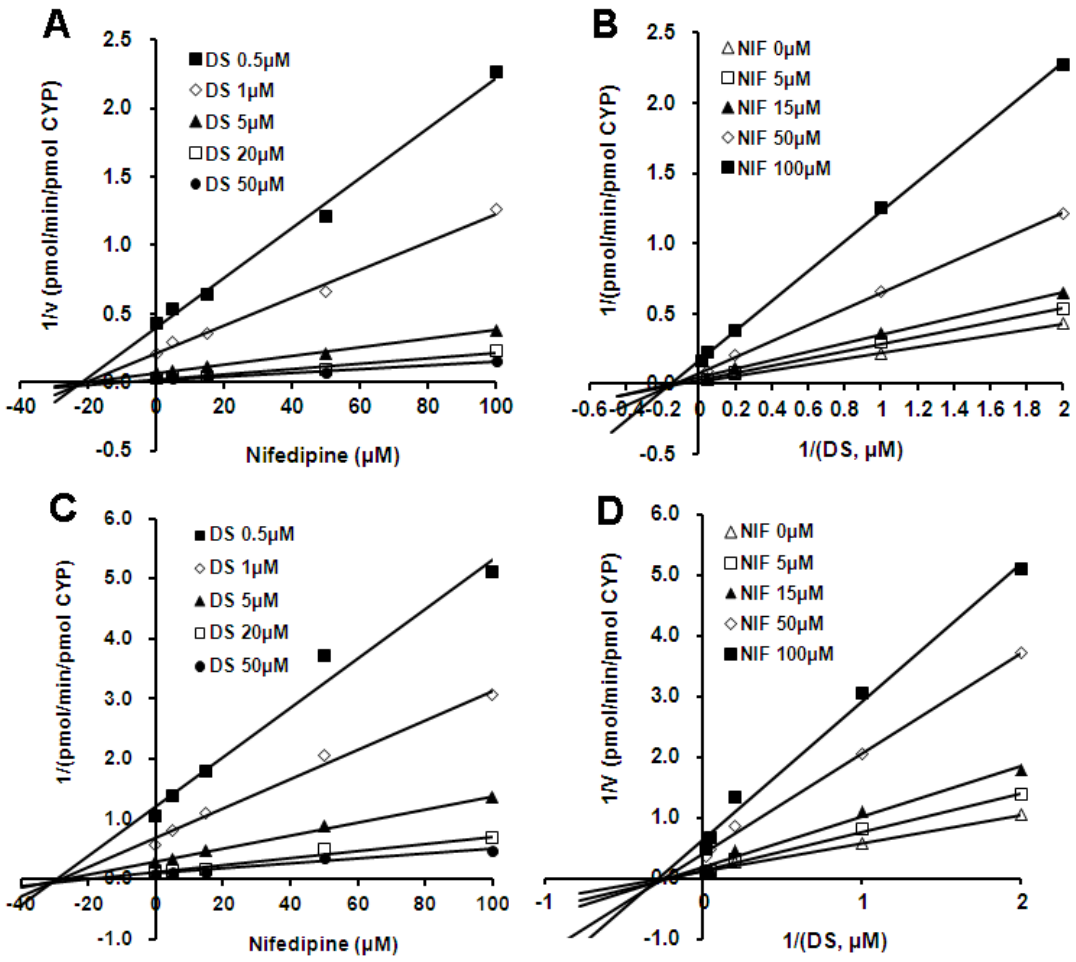
A
1/v (pmol/min/pmol CYP)
Nifedipine (μM)
DS 0.5μM
DS 1μM
DS 5μM
DS 20μM
DS 50μM
B
1/(pmol/min/pmol CYP)
1/(DS, μM)
NIF 0μM
NIF 5μM
NIF 15μM
NIF 50μM
NIF 100μM
C
1/(pmol/min/pmol CYP)
Nifedipine (μM)
DS 0.5μM
DS 1μM
DS 5μM
DS 20μM
DS 50μM
D
1/V (pmol/min/pmol CYP)
1/(DS, μM)
NIF 0μM
NIF 5μM
NIF 15μM
NIF 50μM
NIF 100μM

Figure 5

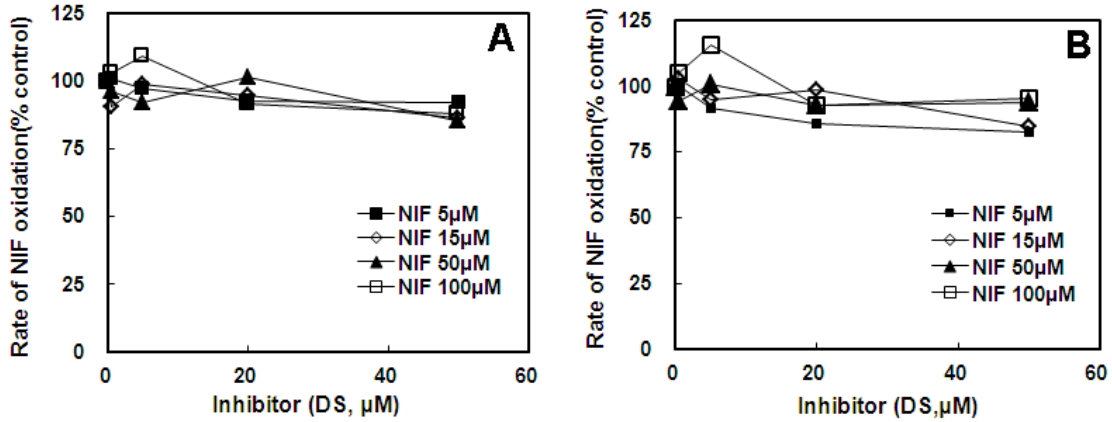
A
B
Rate of NIF oxidation(% control)
Inhibitor (DS, μM)
Inhibitor (DS,μM)
NIF 5μM
NIF 15μM
NIF 50μM
NIF 100μM
0
25
50
75
100
125
0
20
40
60